Graduate School ETD Form 9
(Revised 12/07)

PURDUE UNIVERSITY
GRADUATE SCHOOL
Thesis/Dissertation Acceptance

This is to certify that the thesis/dissertation prepared

By Tianxiu Wang

Entitled DNA Recognition and Cleavage by Phenyl-Benzimidazole Modified Gly-Gly-His-Derived Metallopeptides

For the degree of Master of Science

Is approved by the final examining committee:

Eric C. Long
Chair

Brenda J. Blacklock

Christoph A. Naumann

To the best of my knowledge and as understood by the student in the *Research Integrity and Copyright Disclaimer (Graduate School Form 20)*, this thesis/dissertation adheres to the provisions of Purdue University's "Policy on Integrity in Research" and the use of copyrighted material.

Approved by Major Professor(s): Eric C. Long

Approved by: Martin J. O'Donnell 03/04/2010
Head of the Graduate Program Date

Graduate School Form 20
(Revised 1/10)

PURDUE UNIVERSITY
GRADUATE SCHOOL

Research Integrity and Copyright Disclaimer

Title of Thesis/Dissertation:

DNA Recognition and Cleavage by Phenyl-Benzimidazole Modified Gly-Gly-His-Derived Metallopeptides

For the degree of Master of Science

I certify that in the preparation of this thesis, I have observed the provisions of *Purdue University Teaching, Research, and Outreach Policy on Research Misconduct (VIII.3.1)*, October 1, 2008.*

Further, I certify that this work is free of plagiarism and all materials appearing in this thesis/dissertation have been properly quoted and attributed.

I certify that all copyrighted material incorporated into this thesis/dissertation is in compliance with the United States' copyright law and that I have received written permission from the copyright owners for my use of their work, which is beyond the scope of the law. I agree to indemnify and save harmless Purdue University from any and all claims that may be asserted or that may arise from any copyright violation.

Tianxiu Wang

Printed Name and Signature of Candidate

03/04/2010

Date (month/day/year)

*Located at http://www.purdue.edu/policies/pages/teach_res_outreach/viii_3_1.html

DNA RECOGNITION AND CLEAVAGE BY PHENYL-BENZIMIDAZOLE MODIFIED GLY-GLY-HIS-DERIVED METALLOPEPTIDES

A Thesis

Submitted to the faculty

of

Purdue University

by

Tianxiu Wang

In Partial Fulfillment of the

Requirements for the Degree

of

Master of Science

May 2010

Purdue University

Indianapolis, Indiana

Dedicated to My Parents

ACKNOWLEDGEMENTS

I would like to thank my advisor, Dr. Eric Long, for his encouragement, guidance and support throughout this work. I am also grateful to Dr. Brenda Blacklock and Dr. Christoph Naumann for their service on my thesis committee. I would also like to acknowledge my friends and colleagues at IUPUI for their constructive input and advice, especially Bo Li, her kind help and friendship are greatly appreciated. Special thanks go to Dr. Tax Georgiadis for providing help with syntheses and product characterization. Finally, I would like to thank my parents for their constant support throughout my graduate career. I wouldn't have got it done without their unwavering love.

TABLE OF CONTENTS

Page

Page

Page

LIST OF FIGURES

Figure Page

Figure Page

LIST OF ABBREVIATIONS

Arg	arginine
BI	benzimidazole
BI(+)	amidinium benzimidazole
Boc	*t* –butyloxycarbonyl
bp	base pair
DCM	dichloromethane
DIC	diisopropylcarbodiimide
DMF	*N*,*N*-dimethylformamide
DNA	deoxyribonucleic acid
EDTA	ethylenediaminetetraacetic acid
equiv	equivalent
EtBr	ethidium bromide
Fmoc	fluorenylmethoxycarbonyl
Gly	glycine
His	histidine
HOBt	1-hydroxybenzotriazole
HPLC	high performance liquid chromatography
LC/MS	liquid chromatography-mass spectrometry
Lys	lysine
TFA	trifluoroacetic acid

ABSTRACT

Wang, Tianxiu. M.S., Purdue University, May 2010. DNA Recognition and Cleavage by Phenyl-Benzimidazole Modified Gly-Gly-His-Derived Metallopeptides. Major Professor: Eric C. Long

Metallopeptides of the general form M(II)·Gly_1-Gly_2-His induce DNA strand scission via minor groove interactions. This peptide system can serve as a nucleic acid-targeted cleavage agent – either as an appendage to other DNA binding agents, or as a stand alone complex. In an effort to further our knowledge of DNA recognition and cleavage, a novel series of phenyl-benzimidazole modified Gly-Gly-His-derived metallopeptides was synthesized via solid phase methods and investigated. The new systems allow the formation of additional contacts to the DNA minor groove through the incorporation of a DNA binding phenyl-benzimidazole moiety, thus strengthening the overall binding interaction and further stabilizing the metal complex-DNA association. In addition, how Lys side chains and an amidinium group influence the efficiency of DNA cleavage was also studied. DNA cleavage studies suggested that the phenyl-benzimidazole-modified Gly-Gly-His metallopeptides possess enhanced DNA cleavage abilities. In particular, when amidines are placed on the benzimidazole moieties, these moieties appeared to play an important role in increasing the DNA cleavage activity of the metal complex, most likely through an enhanced electrostatic attraction to the DNA.

CHAPTER1. INTRODUCTION: PEPTIDE-BASED SMALL MOLECULE-DNA INTERACTIONS

1.1 Overview

The DNA minor groove has been an important focus of chemical and biological studies ever since the elucidation of the structure of DNA and its role in the life cycle of a cell. In particular, much effort has been directed toward the development of synthetic DNA binding agents that target this DNA structure feature due to their potential as anti-cancer, anti-viral, and antimicrobial drugs.[1] Examples include the quinoxaline family[2] of DNA intercalators, minor groove-binding molecules such as netropsin and distamycin,[3-4] and the bleomycin group[5] of DNA cleavage agents. The binding of such compounds to the DNA minor groove usually involves a combination of weak intermolecular forces, such as electrostatics, van der Waals forces, and hydrogen bonding. As a general rule, minor groove binding compounds exert their biological impact through the disruption of normal cellular functions by binding at or near promoter regions of genes thus altering transcription;[1] additionally, DNA minor groove binders can also disrupt DNA replication and, in the case of cleavage agents, lead to DNA damage.

The rational design of DNA binding agents often derives from known structural features of DNA-targeted natural products. Recently, for example, polyamides[6] which were designed based on the natural products, netropsin and distamycin, have been demonstrated to target DNA selectivity through a “Pairing Code”.[7] Additionally, benzimidazole derived ligands[8-9] have displayed exceptional DNA binding abilities; these findings have broadened our vision with regard to potential future designs for DNA minor groove binding compounds.

In addition to simply binding to the minor groove of DNA, clinically-employed antitumor agents such as the bleomycins can also induce DNA strand scission; the bleomycins cleave DNA through C4’-H abstraction[10] when complexed with certain transition metals. Similarly, our laboratory has exploited M(II)·Gly_1-Gly_2-His-derived metallopeptides (Figure 1.1) as stand alone complexes to better understand amino acid- and peptide-nucleic acid recognition principles through DNA cleavage chemistry. In general, tripeptides can utilize a metal center to organize the linear peptide structure and to provide a platform that supports redox activity leading to DNA cleavage.

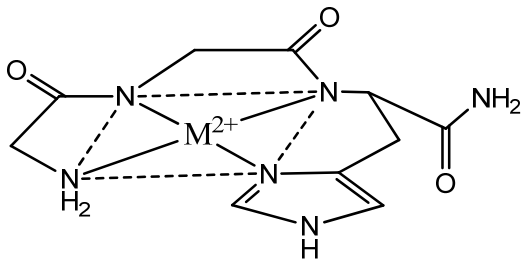

Figure 1.1. General structure of an M(II)·Gly_1-Gly_2-His-derived metallopeptide.

Given their amino acid compositions, the DNA targeting of these metallopeptide systems can be modulated by[10]: (1) the inclusion of certain amino acids and (2) the stereochemistry at each α-carbon[10] leading to varied levels of DNA cleavage activity and site selectivity. Similar to the DNA cleavage chemistry of the bleomycins, direct DNA strand scission also occurs via C4'-H abstraction through an interaction between the activated metallopeptide complex and the floor of the minor groove.[11] However, these metallopeptides alone are not tight DNA binders. Thus, a new design for Gly-Gly-His-derived metallopeptides was investigated in this thesis work. These new designs are comprised of two parts: (1) metallopeptides as studied previously[10] and (2) benzimidazole moieties as used in many DNA ligand designs.[12-14] Therefore, this series of compounds was generated with the aim of targeting DNA with higher efficiency.

1.2 DNA Structure

Ever since the structures of nucleic acids were revealed in the early 1950s, they have become popular targets for molecular recognition studies. Deoxyribonucleic acid (DNA), which acts as a genetic archive, is composed of nucleobases (purines, pyrimidines), deoxyribose sugars, and phosphates. In the primary DNA structure, phosphodiester-linked deoxyribose units form the backbone of each DNA strand and the double helix is made from two such strands winding helically around each other in an antiparallel fashion. The interior of the DNA helix is composed of stacked base pairs (A·T, G·C) which are attached to the C1' on the sugar rings via an *N*-glycoside bond and interact with each other via hydrogen bonds to form Watson-Crick base pairs (Figure 1.2).

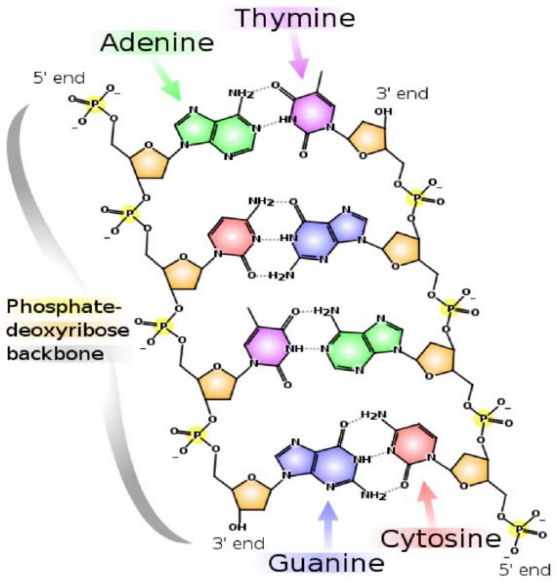

Figure 1.2. Primary structure of DNA.

It is well-known that DNA adopts three main conformations, the A-form, B-form and Z- form (Figure 1.3). B-form DNA is the most common and exists under physiological conditions. Generally speaking, the double helical structure of B-DNA conforms to the features of canonical Watson-Crick DNA: a right-handed double helix with approximately ten nucleotides per helical turn. Compared to B-DNA, A-DNA is wider and has base pairs inclined to its helix axis instead of being perpendicular to it. Z-DNA, on the other hand, is a left-handed helix whose repeat units are dinucleotides and exhibit a characteristic “zigzag” backbone.[15] The conformation DNA adopts depends on the hydration level, DNA sequence and chemical modification of the bases.[16] Moreover, the DNA molecule can adapt itself to the environment and therefore, it can exhibit several different conformations in different segments.[15]

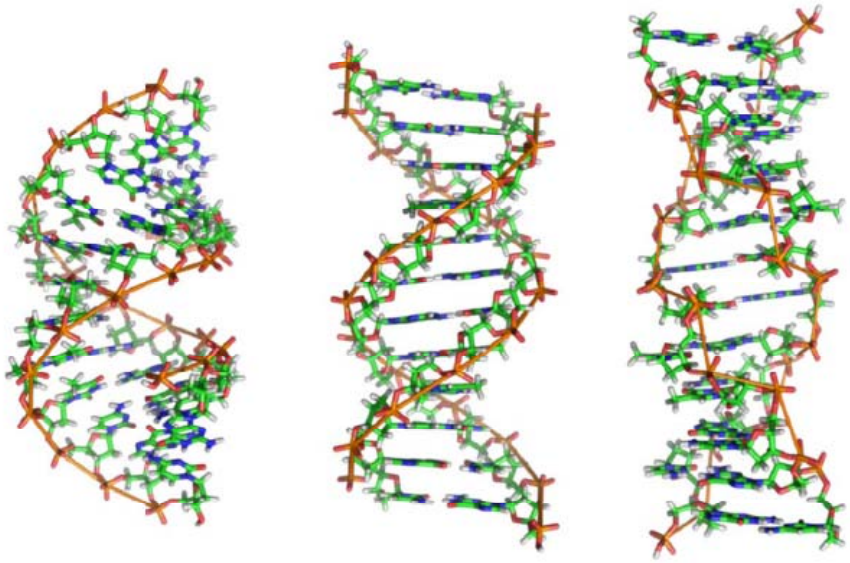

Figure 1.3. The structures of A, B, Z-DNA (from left to right).

Due to the asymmetry of the *N*-glycoside connection to the Watson-Crick base pairs, there are two unequally sized grooves formed in B-form DNA, designated the major and minor grooves. As they are named, the major groove is wide, while the minor groove is narrow (Figure 1.4 A).[17] The edges of base pairs constitute the floor of the grooves and present different hydrogen bonding acceptor and donor patterns to a possible ligand. Indeed, a closer look at the grooves of DNA reveals a basis for DNA sequence recognition mechanisms (Figure 1.4 B). For the major groove, the edges of A·T and G·C base pairs provide three possible hydrogen bonding sites: there are two hydrogen bond acceptors (guanine-N7 and guanine-O4) and one hydrogen bond donor (cytosine-N4) from G·C pairs; similarly, two hydrogen bond acceptors (adenine-N7 and thymine-O4) and one hydrogen bond donor (adenine N6) are presented by A·T pairs. In addition, the methyl group of T provides a potential van der Waals interaction. Large molecules, such as proteins which have more functional groups, generally identify bases in the major groove of DNA leading to their site-specific DNA binding.

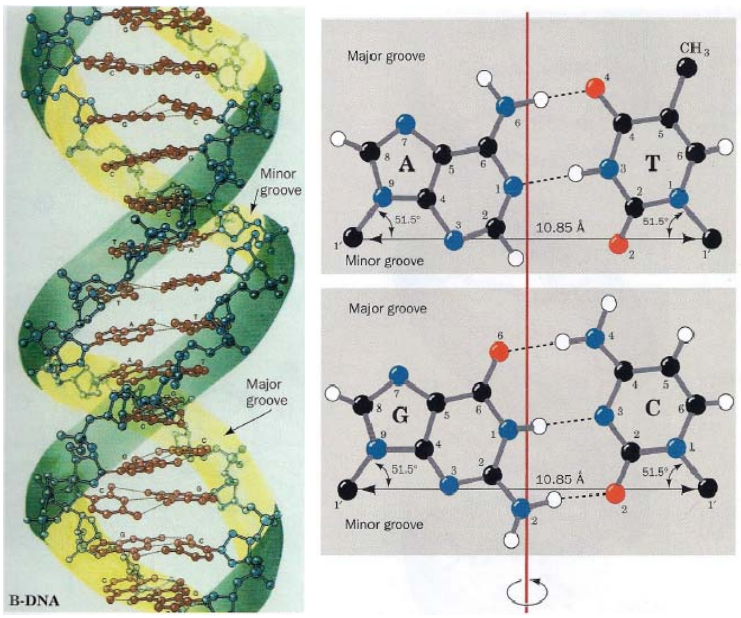

A B

Figure 1.4. Three dimensional structure of B-DNA (A); Watson-Crick base pairs (B).

In comparison, the minor groove presents fewer functionalities for nucleobase recognition. There are only three accessible hydrogen bonding sites at a G·C base pair and two hydrogen bond acceptors at adenine-N3 and thymine-O2 of an A·T site. Although it seems that the edge of G·C is more favorable than those of A·T, several studies have demonstrated that many binding agents prefer A·T sites over G·C sites, suggesting that hydrogen bonding is not a dominant factor for sequence discrimination of the minor groove. Indeed, electrostatic potential also plays an important role: a run of A·T base pairs has the greatest negative potential at the floor of the minor groove, whereas, G·C sequences have the greatest positive potential.[1] This likely explains why cationic agents prefer to bind A·T rich regions. Moreover, X-ray studies suggest that the exocyclic N2 amino group of guanine is often a steric block to minor groove binding.[18] As a consequence of the structure of the narrow minor groove, low molecular weight ligands with specific structures can be accommodated.

In summary, much effort and progress has been made to further our understanding of the structural features of DNA biomacromolecules. The numerous binding sites displayed on the surface of DNA and the knowledge of known binders (proteins and low molecular weight compounds) continuously inspire scientists to design and construct novel molecules with enhanced DNA affinity and specificity. Given the topic of this thesis, the following sections will focus on low molecular weight ligand-DNA interactions located in the minor groove.

1.3 DNA-Small Molecule Interactions

In general, a combination of electrostatic interactions, hydrogen bonding, hydrophobic interactions, wan der Waals contacts, and steric forces combine to influence the mode of ligand binding.[19] Koshland proposed the 'induced fit' model which, when applied to DNA recognition, suggests that both the DNA helix and a potential binder might experience some conformation changes upon their interaction. Distortions of DNA structure (bending, unwinding, lengthening, etc.) are observed in many ligand-DNA complexes. For example, intercalation into DNA usually causes significant local structural changes of the duplex; while groove binding, at times, can significantly perturb the DNA structure.[19]

The binding of small molecules to the minor groove can also lead to DNA cleavage. This process typically involves one of the following pathways: (1) oxidation at the deoxyribose sugar ring by abstracting a hydrogen atom which results in the fragmentation of the sugar; (2) modification of a nucleobase; and (3) the hydrolysis of the phosphodiester backbone.[20] In all these cases DNA polymer strand fragmentation can occur.

1.3.1 DNA Intercalators

Intercalation occurs when a planar, aromatic moiety slides between two adjacent stacked DNA base pairs.[21] Intercalation changes the base pair spacing from 3.4 Å to 6.8 Å and induces local structural changes to the DNA such as helix unwinding and B-form to A-form transitions (Figure 1.5). These changes can alter DNA-based processes. Therefore, some intercalators such as ethidium bromide (Figure 1.6) are also potent mutagens. Similarly, due to their tight association with DNA, many intercalators have clinical efficacy and have been used as chemotherapeutic treatments to inhibit DNA replication in rapidly growing cancer cells.

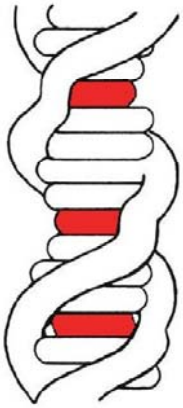

Figure 1.5. DNA intercalation.

Several intercalators such as ethidium bromide (Figure 1.6) and thiazole orange are used as non-specific intercalating agents that display enhanced fluorescence upon DNA binding. The intense fluorescence of these agents upon DNA binding derives from electronic perturbations in the ligand and result from the release of fluorescence quenching water as well as the stabilization of overlapping π-systems. The application of fluorescent intercalators to examine the DNA binding characteristics of other molecules is particularly useful.[22-23] in addition, ethidium bromide is employed to visualize the presence or the location of DNA fragments in agarose gel electrophoresis.[24-25]

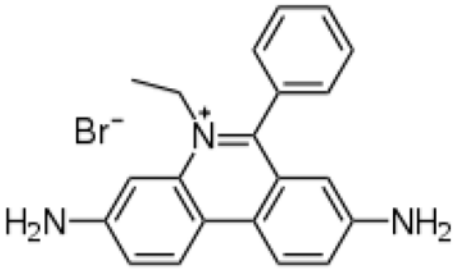

Figure 1.6. Structure of ethidium bromide.

Along with monointercalators such as ethidirm bromide, there are also many natural bisintercalators, for example, the quinoxaline antibiotics (echinomycin) (Figure 1.7).[2] Beyond bisintercalators, synthetic efforts have led to tris- and tetraintercalators or even polyintercalators to cover longer DNA sequences.[26] Although many intercalators do not exhibit high levels of DNA sequence site selectivity, studies do indicate that they generally favor insertion into G·C rich regions.[27] This preference points out that π-π overlap plays an important role in DNA Intercalation.

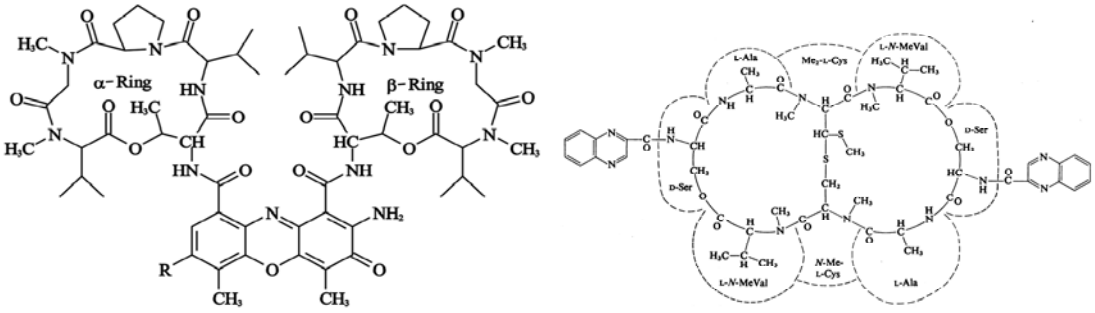

A B

Figure 1.7. Chemical structures of a monointercalator (A) and a bisintercalator (B).

1.3.2 DNA Minor Groove Binders

In addition to intercalative binding, the 3D structure of DNA duplexes also allow contacts in their major and minor grooves. As a general rule, protein recognition occurs

mainly through the major groove while small molecules generally prefer minor groove binding. Additionally, many minor groove binders exhibit an A·T preference. In order to better understand favored binding in the DNA minor groove, several structural factors must be taken into consideration as discussed below.

The electrostatic potential along a DNA sequence is sequence-dependent, with a run of A·T base pairs having a greater negative potential than a run of G·C base pairs at the floor of the minor groove. This is due to the presence of electro-rich thymine O2 and adenine N3 (Figure 1.8).[1] This feature makes A·T rich sequence more attractive to low molecular weight agents which carry positive charges. Agents such as netropsin and distamycin represent classic examples of minor groove binders and contain at least one positively charged moiety. Similarly, synthetic minor groove binding ligands are typically designed to incorporate at least one positively charged moiety to improve binding affinity

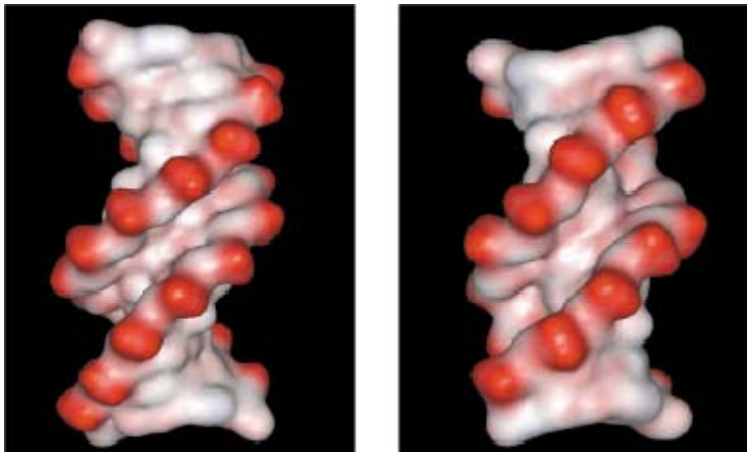

A B

Figure 1.8. View of the electrostatic potential surface of DNA, where red represents positive potential. The narrow A·T minor groove (A); The wide G·C minor groove (B).

As mentioned before, DNA groove widths vary along the helix. G·C rich regions in the minor groove are about 6 Å wider than the corresponding A·T rich regions. The

narrowed groove width in A·T rich regions can provide hydrophobic contacts for flat, curved small molecules.[28] Also, the narrowed A·T rich minor groove can align a small molecule in such a way as to permit the hydrogen bonding groups to be exposed directly to the floor of the groove where they can interact with hydrogen bond acceptors.[1] In addition, the curvature of the A·T rich minor groove complements the overall shape of many small binding ligands very well, whereas the floor of G·C tracts have discontinuities arising from the presence of the guanine exocyclic 2-amino group.[1]

The following section introduces several DNA minor groove binding molecules. Information obtained from their study can help further our knowledge of DNA recognition principles and guide the design of next generation agents.

1.3.2.1 Netropsin and Distamycin

Netropsin and distamycin represent extensively studied natural products derived from *Streptomyces netropsis* and *Streptomycete distallicus*[29] and are well-known for their A·T selective DNA binding properties. As shown in Figure 1.9, the molecules are crescent shaped bi- and tripeptides containing pyrrole rings linked by amide bonds.[30] So far, over 20 high-resolution structures of netropsin-DNA and distamycin-DNA complexes obtained by NMR and X-ray crystallography have been reported.[31,3,4] Also, quantitative footprinting methods have been employed to analyze their sequence preferences.[32]

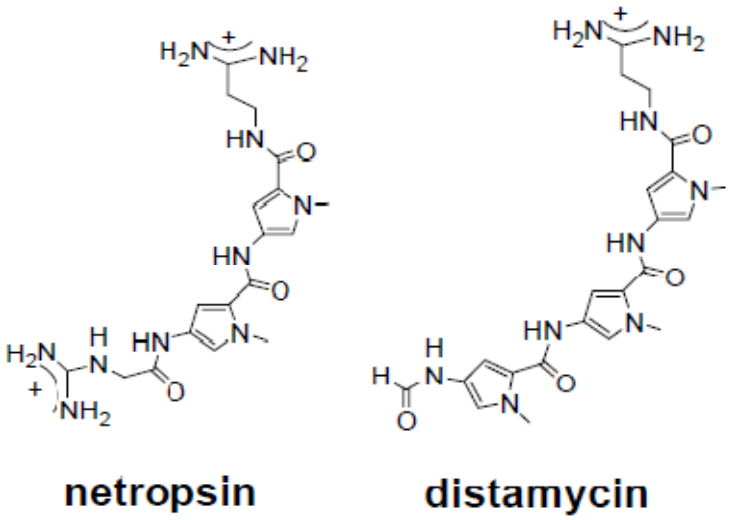

Figure 1.9. The structures of netropsin and distamycin.

These investigations have revealed the detailed mechanisms by which these antibiotics bind to and recognize double-stranded DNA.[33] As noted, both netropsin and distamycin possess propylamidinium groups at their C-termini and netropsin possesses a guanidinium at its N-terminus (or with distamycin a formylated N-termini). These positively charged tails provide electrostatic attractions to DNA and facilitate the delivery of the ligands to the electronegative minor groove. Conceptually, the binding process may thus be divided into two parts. First, the groove binding agents undergo a hydrophobic transfer from bulk solution into the DNA minor groove,[34] localization in the minor groove then promotes the formation of short range affinity-enhancing interactions: once in the minor groove, van der Waals attractions and hydrogen bonds are formed between the ligands and the floor of minor groove. The inherent crescent shape of these drugs also complements the minor groove curvature very well, which leads to deep penetration and close van der Waals contact. Moreover, the amide hydrogens of the *N*-methypyrrolecarboxamides of these agents form bifurcated hydrogen bonds with the N3 of adenine and the O2 of thymine on the floor of minor groove.[30] This favored interaction

between the amide hydrogens and the A·T base pair edges results in preferential A·T binding. An illustration of the hydrogen bonds formed between netropsin and the minor groove is presented in Figure 1.10.[35]

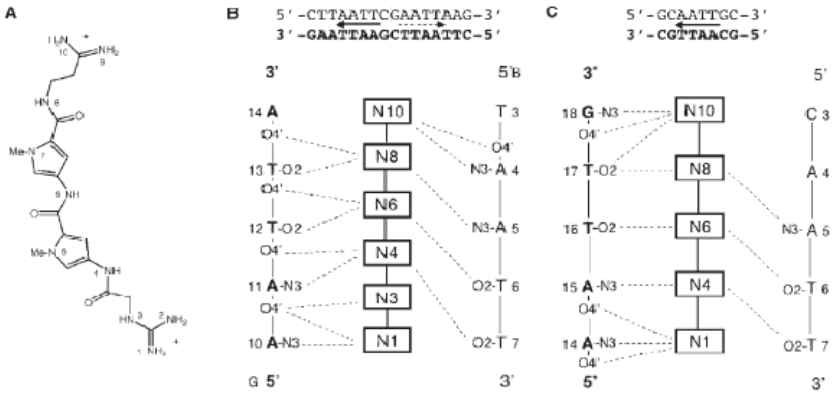

Figure 1.10. Netropsin-minor groove hydrogen bonding interactions.

1.3.2.2 Polyamides

Given the modular nature and DNA binding selectivities of netropsin and distamycin, many minor groove binders have been designed based on the architecture of these lead compounds. Initially, the strategy intended to extend the length of these groove binding agents in hopes of targeting longer DNA sequences.[34] However, simply connecting additional *N*-methypyrrolecarboxamide residues together or joining two netropsin molecules doesn't make them efficient DNA binders because of their length. The second phase synthetic effort involved replacing the carboxamide bond in netropsin or distamycin with shorter keto or amino linkages.[34] This new strategy also introduced imidazole, furan rings and other heterocycles to recognize G·C tracts. Based on these changes, a family of compounds called lexitropsins was synthesized by Lown and

coworkers.[36-39] The ability of lexitropsins to read G·C base pairs embedded in A·T rich regions on DNA arises from the hydrogen bond acceptor groups located on these heterocyclic substitutions, as illustrated in Figure 1.11.[36] However, lexitropsins showed reduced overall DNA binding affinity and relatively low G·C specificity.

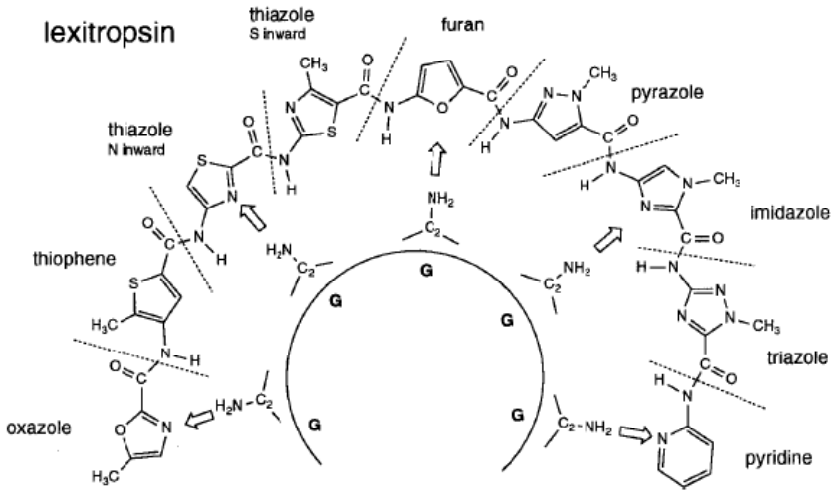

Figure 1.11. Proposed model of the interaction of a lexitropsin with guanine residues in DNA.

Following the above work, the discovery[40] in 1989 that the minor groove of A·T rich DNA could accommodate two distamycin molecules associated in an antiparallel side-by-side orientation inspired the design of dimeric systems.[7] Shortly after that, NMR studies demonstrated that two synthetic polyamides can fit side-by-side into DNA minor groove to permit both to interact with base pairs via hydrogen bonding (Figure 1.12).[41-42] In addition, it was found that the sequence selectivity and geometry of such a ligand-DNA complex could be optimized by choosing appropriate pairs of ligand molecules with complementary recognition properties.[34] Thus, a new dimer system could be engineered to distinguish G·C base pairs from C·G base pairs, and A·T base pairs from T·A base pairs, the latter could be achieved simply by utilizing the lone electron pairs on the O2 of

thymine. Moreover, covalently linking of two DNA reading polyamides avoids the ambiguity of slipping within the minor groove and 'locks' individual ring pairings in a predictable manner.[42]

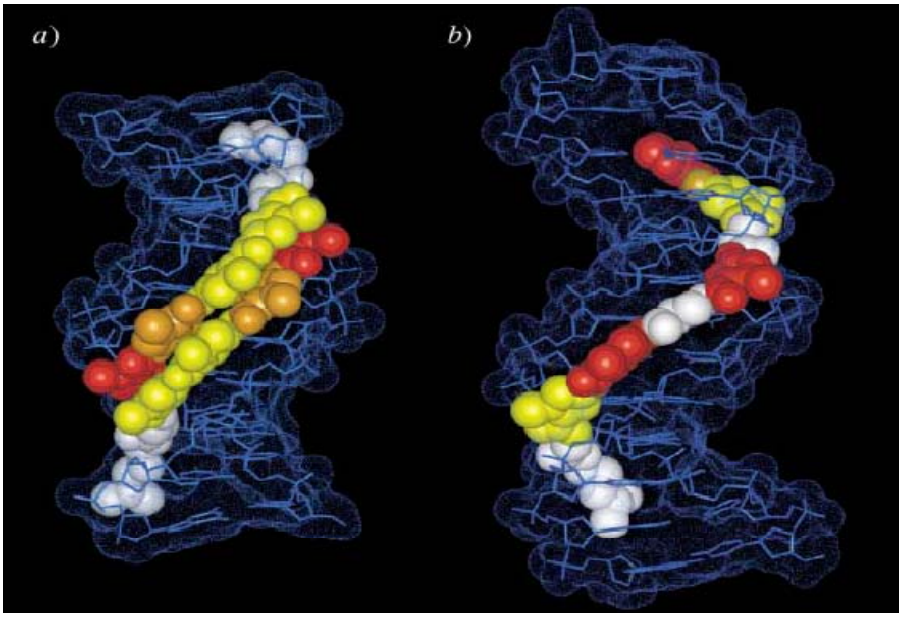

Figure 1.12. Structures of polyamides bound to DNA: a) 2:1 motif; b) 1:1 motif.

Based on the above findings, Dervan *et al.* have developed a series of synthetic polyamide containing pyrrole-imidazole (Py-Im) moieties that can specifically recognize virtually any DNA sequence.[6] These DNA-binding polyamides mainly consist of three central blocks, *N*-methylimidazole (Im), *N*-methypyrrole (Py), and *N*-methyl-3-hydroxypyrrole (Hp) to form crescent 'hairpin' molecules to target DNA sequences (Figure 1.13). Further, the introduction of a bulkier 3-hydroxypyrrole brings steric destabilization of binding to adenine and allows the hydrogen donor penetrating into the groove to interact with O2 of thymine, thus discriminating A·T base pairs from T·A base pairs. Therefore, all four base pairs can be identified: Im/Py targets G·C; Py/Im targets C·G; Hp/Py targets T·A; Py/Hp targets A·T, this is referred to as the Pairing Code (Figure 1.13). Studies also found that polyamides containing an N-terminal formamido group

displayed enhanced DNA binding ability.[43-44] As a result, this new generation of polyamides extended DNA sequence recognition sites up to 16 base pairs.[45] Furthermore, hairpin polyamides can exhibit affinities and specificities for DNA comparable with transcription factors and other DNA binding regulatory proteins.[46]

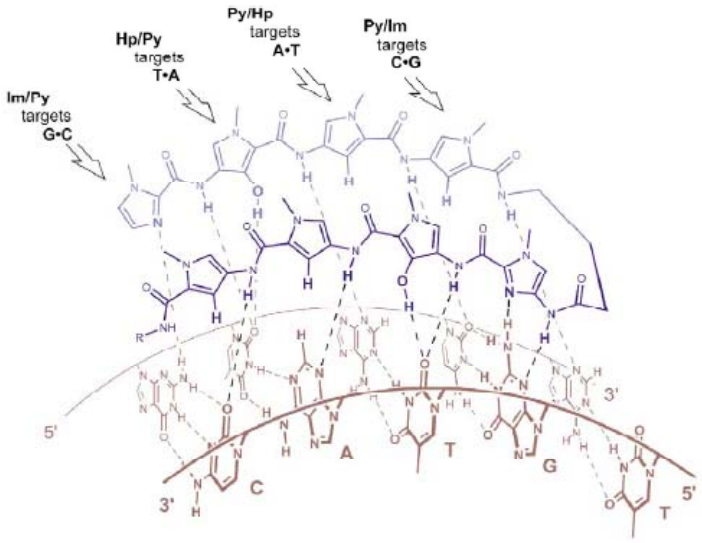

Figure 1.13. Illustration of Dervan's "Pairing Code".

More recently, efforts have been devoted to developing heterocycles that are capable of cooperatively pairing with each other to recognize DNA base pairs in the minor groove.[47] Towards this end, the incorporation of fused heterocycles such as benzimidazole has been investigated. Notably, benzimidazoles appear in the structures of some DNA minor groove binders, for example, Hoechst 33258, which can recognize sequences such as 5'-WGGGGW-3' with high affinity.[48] The benzimidazole moiety integrated into the hairpin polyamide templates presents hydrogen donating groups to the floor of DNA minor groove, thus maintaining similar DNA recognition properties. In addition, hydroxybenzimidazole (Hz) can be used to replace hydroxypyrrole which degrades over time in the presence of acid or free radicals.

Certain designed polyamides are able to influence gene expression. An eight ring hairpin Py-Im polyamide which binds six base pairs was reported to inhibit the binding of the transcription factor TFIIIA, thus suppressing the transcription of 5S genes.[49] In another study, androgen-induced expression of prostate-specific antigen and several other androgen receptor (AR)-regulated genes are inhibited by cell-permeable polyamides.[50] Polyamides offer an alternative approach to antagonizing AR activity. In addition, the programmability of polyamides may allow more powerful inhibition of predetermined target genes.[51]

1.3.2.3 Benzimidazole-Based Systems

Hoechst 33258 is comprised of two benzimidazole groups linked in a head-to-tail manner with a phenol head and *N*-methylpiperazine tail (Figure 1.14). It is primarily used as a fluorescent DNA stain, which can be excited by ultraviolet light at around 350 nm to emit a blue/cyan fluorescence light at around 461nm upon binding to dsDNA. DNA footprinting and biophysical studies have shown that Hoechst 33258 binds selectively to A·T sequences, with a binding site size of 4-5 bases.[1] As a DNA binder, Hoechst exhibits antitumor activity[31] and has been in phase I/II clinical trials against pancreatic carcinomas;[52] however, this candidate was abandoned due to its toxicity.[1]

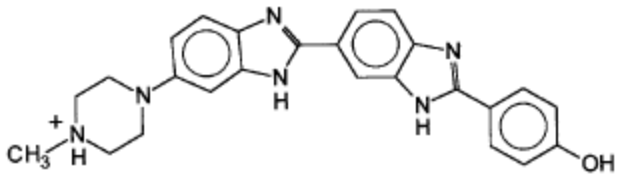

Figure 1.14. Structure of Hoechst 33258.

Crystal structure analyses and NMR studies[53-54] of Hoechst 33258 complexed to various oligonucleotide duplexes have revealed the binding mode of the drug in the DNA minor groove. The ligand adopts a crescent conformation and makes extensive van der Waals contacts with the backbone and base atoms; the planar benzimidazole moiety,[55] orients parallel to the groove direction and forms bifurcated hydrogen bonds to the A·T base pairs in a fashion very similar to that of netropsin;[56] the bulky *N*-methypiperazine ring of the drug, most of the time, is located in a wider G·C region without participating in a hydrogen bond.[53,57]

A number of Hoechst 33258 analogues that bind certain extended A·T sequences in DNA[8-9] have been designed and synthesized (Figure 1.15). The study of these compounds introduces a new point of view on small molecule-DNA interaction principles, one which is slightly different from the canonical models exemplified by netropsin and distamycin.

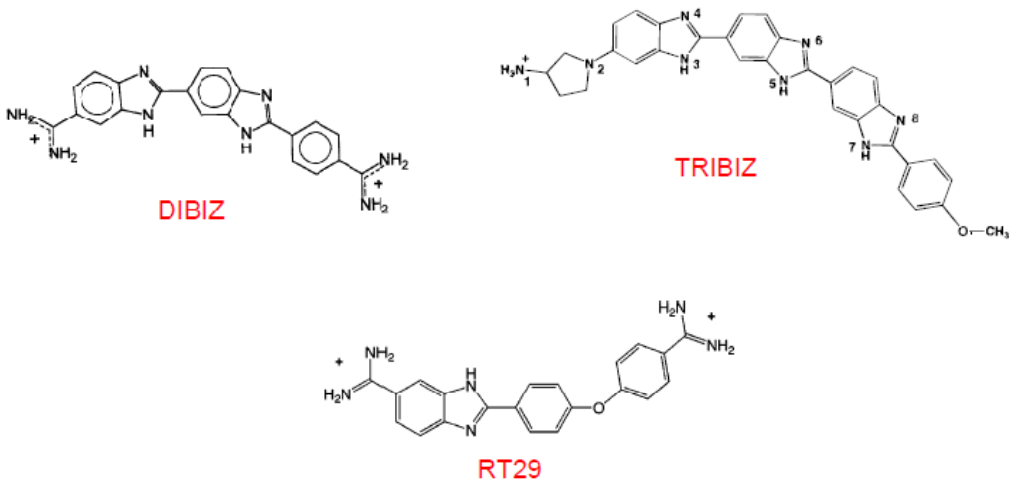

Figure 1.15. Structures of some benzimidazole derived DNA binding agents.

While most minor groove binder designs focus on the development of concave inner-faced ligands which complement the shape of the minor groove floor,[9] as shown in Figure 1.15, none of the three compounds satisfies this criterion despite their good DNA binding properties. For example, with RT29, the diphenyl ether moiety is over-curved compared to agents such as netropsin and distamycin. Consequently, these flat compounds should fail to position their functional groups in an effective way for hydrogen bonding in the minor groove of DNA. Surprisingly, on the contrary, the ligands exhibit enhanced binding affinity relative to their parent compound Hoechst 33258.[8-9] To explain their binding, X-ray studies revealed that the ligands undergo conformational changes, such as twists and distortions to follow the helical curvature of the minor groove and place the functional groups in closely optimized positions for interaction with DNA.[8] Additionally, water molecules play an important role in stabilizing drug-minor groove interactions. The drug molecules recruit water molecules at their termini to bridge with additional base pair edges.

Another structural alteration involved the introduction of cationic amidinium groups into the design. In addition to making the ligands attractive to the DNA minor groove, amidinium nitrogens are also observed to participate in hydrogen bonding with A·T base pairs in the minor groove.[35,58-59] In fact, aromatic diamidines have drawn intensive attention due to their broad-spectrum antimicrobial activities which are believed to result from the minor groove binding of these type of compounds.[60] In short, effective subunit phasing upon DNA minor groove binding, in combination with extra hydrogen bonds established from the amidine groups of these benzimidazole-derived compounds make them strong additions to any DNA binding ligand designs.

1.3.3 DNA Cleavage by Natural Products

Considerable effort has been put into studying and designing ligands that not only bind DNA, but are also capable of modifying the DNA helix. Among such agents, the bleomycins are a family of glycopeptide derived natural products first isolated from *Streptomyces verticillus* by Umezawa *et al.* in 1966.[5] Soon after their discovery, bleomycins were used in the treatment of several neoplastic diseases including squamous cell carcinomas, malignant lymphomas and ovarian cancer.[61-62] The bleomycin group contains over 200 closely related compounds that differ only in their sugar moieties and positively charged C-termini.[61] When used as an anti-cancer drug, the administered forms are primarily bleomycin A_2 and B_2 and the therapeutic utility of the bleomycins is believed to derive from their ability to mediate DNA strand scission, a transformation that is metal ion and oxygen dependent.[62] Recent studies of bleomycin have focused on their structures and DNA binding selectivity.

As presented in Figure 1.16, the structure of bleomycin can be separated into three regions: (1) the pyrimidine, β-amino alanine and β-hydroxyimidazole moieties, which constitute the core metal-binding peptide that is responsible for DNA cleavage and site recognition; (2) the positively charged bithiazole moiety that increases DNA binding affinity; and (3) the glucose and carbamoylated mannose carbohydrate residues, which are believed to aid in the cellular uptake of the drug and increased stabilization upon DNA binding. The functions of these domains were evaluated by studying several bleomycin analogues: studies demonstrated that the lack of sugar, peptidyl linker or bithiazole tail does not affect the sequence-selectivity of these compounds, which supports the notion that the metal binding domain plays an important role in binding to DNA.[63] In addition, it was proposed that the drug-DNA binding is initiated via bithiazole

intercalation in cooperation with alignment of the metal binding domain on the floor of the minor groove.[61] Thus, the binding affinity and cleavage selectivity derives from the metal binding domain in cooperation with the bithiazole tail.

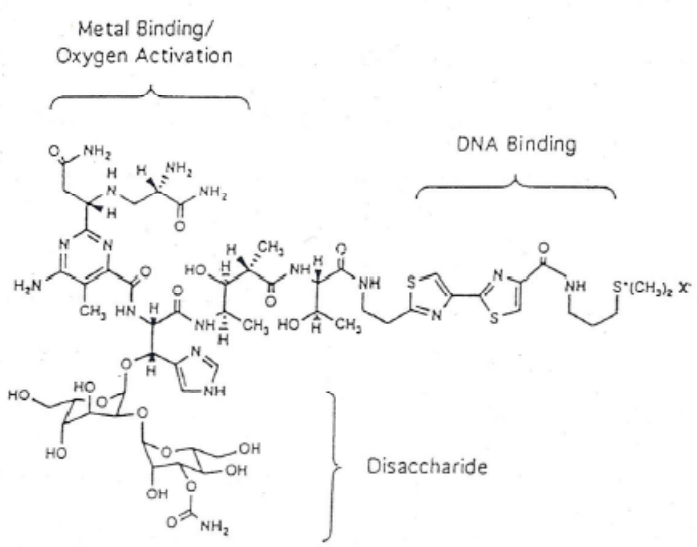

Figure 1.16. Structure of bleomycin A_2.

The best characterized property of bleomycin is certainly its ability to mediate the degradation of DNA substrates.[64] This process has been established by analyzing fragments from various bleomycin-DNA interactions. Bleomycin induced DNA degradation requires the presence of a redox-active metal ion such as Fe(II), as well as molecular oxygen.[65] Upon their combination, the formation of an activated complex (Figure 1.17) leads to direct DNA strand scission at 5'-GC or 5'-GT steps which were identified as the preferential DNA cleavage sites of bleomycins via a C4'-H abstraction pathway.[61] Along with DNA cleavage, the bleomycins also mediate lipid peroxidation, membrane damage and oxidative RNA degradation.[61,66]

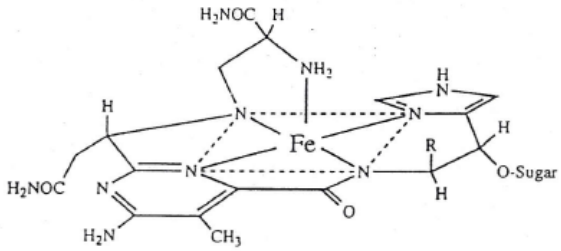

Figure 1.17. Structure of the bleomycin metal binding domain.

In addition to Fe(II), other transition metals including Cu, Co, Mn, Ni, Ru, V and Zn also bind to bleomycin as cofactors.[61] The resultant metallobleomycins are not only structurally different from each other, but also have different DNA recognition and modification properties.[62] Given its metallopeptide core metallobleomycin served as a control in our investigations.

1.4 Metallopeptide-DNA Interactions

1.4.1 Gly-Gly-His-Derived Metallopeptides

Metallopeptides of the general form Cu(II)·or Ni(II)·Gly-Gly-His, where Gly can be any α-amino acid, have historically served as models of the Ni(II) and Cu(II) transport domains of the serum albumins.[67] With Cu(II) or Ni(II) at physiological pH, peptide complexation occurs through chelation of the histidine imidazole nitrogens, two intervening deprotonated amide nitrogens and the terminal α-amine, as shown in Figure 1.18.[10] This peptide was found to bind Cu(II) and Ni(II) in a 1:1 complex with extremely high affinity (K_D values on the order of 10^{-16} M). For our purposes, the square-planar structure which is somewhat similar to the metal binding domain of the metallobleomycins, can generate oxidants that cause DNA strand scission. Indeed, it

has been reported that Cu(II)·Gly-Gly-His + ascobate induced DNA strand scission and showed cytotoxic activity against Ehrlich ascites tumor cells.[68]

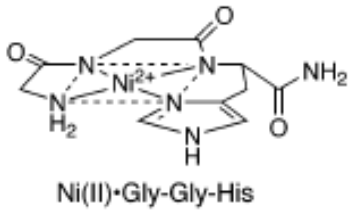

Ni(II)•Gly-Gly-His

Figure 1.18. Structure of Ni(II)·Gly-Gly-His.

1.4.2 DNA Cleavage Analyses

Our research group determined that when activated with equimolar Oxone ($KHSO_5$), magnesium monoperoxyphthalic acid, or hydrogen peroxide at physiological pH, Ni(II)·Gly-Gly-His induced selective, direct DNA strand scission via a nondiffusible oxidant, likely a peptide-bound Ni(III)-HO· or Ni=(IV).[69] Furthermore, our laboratory also identified the DNA products resulting from metallopeptide cleavage. It was found that the 5'- and 3'- termini formed were consistent with the chemistry of C4'-H abstraction.[10] Thus, the metallopeptides are not only structurally similar to the DNA binding domain of Fe(II)·bleomycin, but also parallel the activity of it, that is, causing DNA degradation by C4'- hydrogen abstraction in the minor groove via two different pathways (Figure 1.19): (1) formation of keto-aldehyde abasic lesions and loss of free nucleobase, indicating the formation of a C4'-hydroxyl intermediate and (2) direct DNA strand scission and the release of 5'-phosphorylated termini, 3'-phosophoroglycolate termini and nucleobase propenals, suggesting the formation of a C4'-hydroperoxyl intermediate.[10,69]

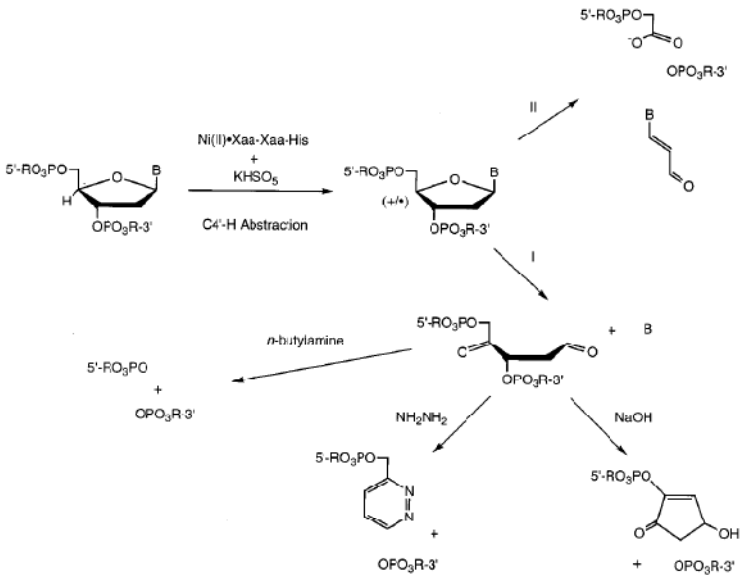

Figure 1.19. Pathways of deoxyribose-based DNA degradation by Ni(II)·Gly_1-Gly_2-His metallopeptides.

To further understand metallopeptide-DNA interactions, Lys and Arg substituted tripeptides that impart a net positive charge to the system for an increased electrostatic interaction with the DNA backbone, were investigated. In particular, peptides with Lys or Arg incorporated into the Gly_1 position (Figure 1.20 A) were found to have DNA cleavage activities at least three-fold higher than that of the neutral Ni(II)·Gly-Gly-His template and become highly focused to A·T rich regions.[10] The DNA-binding mode of Cu(II)·Xaa-Gly-His metallopeptides (where Xaa is Gly, Lys or Arg) has also been characterized by DNA fiber EPR spectroscopy and molecular modeling. These studies revealed that the metal complex binds with its equatorial plane oriented 40℃ relative to the DNA helix axis in the minor groove.[70] Recently, one- and two- dimensional NMR methodologies and molecular simulations were carried out using the A·T rich Dickerson oligonucleotide, $d(CGCGAATTCGCG)_2$, and Ni(II)·Arg-Gly-His in an effort to more precisely define the DNA association characteristics of Gly-Gly-His derived metallopeptides.[67] As presented in Figure 1.20,[67] the results indicated that the His imidazole N-H, the N-terminal peptide

amine and the Arg side chain are major determinants of minor groove recognition by functioning as hydrogen bond donors to the O2 of thymine or N3 of adenine nucleotides.

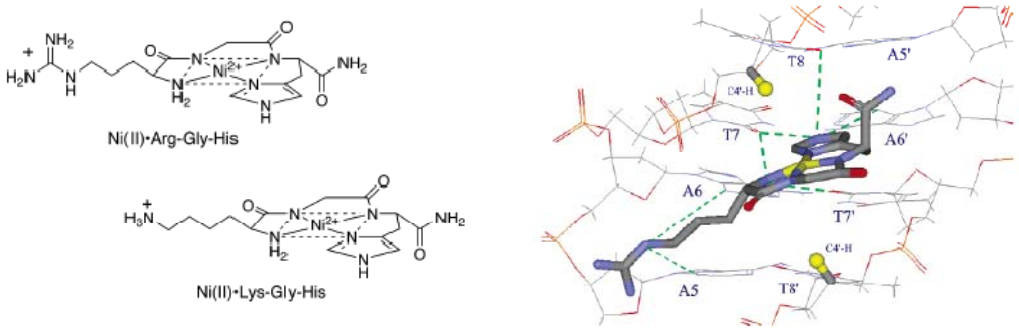

A B

Figure 1.20. Structures of Ni(II)·Arg-Gly-His and Ni(II)·Lys-Gly-His (A); Minor groove binding by Ni(II)·Arg-Gly-His with the O2 of thymine and N3 of adenine (B).

Furthermore, the average structure of Ni(II)·L-Arg-Gly-His produced from molecular dynamic simulations was found to have a surprising correspondence with netropsin and Hoechst 33258 (upon structural studies with the same AATT oligonucleotide) (Figure 1.21), suggesting that these low molecular weight metallo-peptides can mimic natural drug structural strategies for DNA minor groove binding.

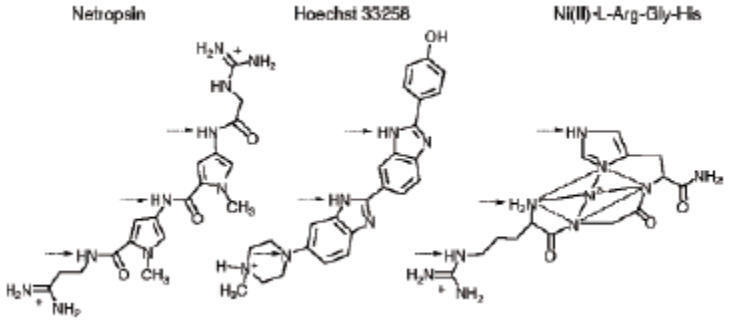

Figure 1.21. Comparison of the structure of Ni(II)·L-Arg-Gly-His to netropsin and Hoechst 33258, arrows indicate locations of potential hydrogen bond donating groups.

1.4.3 Determination of DNA Cleavage

An established plasmid DNA cleavage assay[71] was employed to characterize the overall cleavage activity of these metallopeptides. In such a study, supercoiled Form I DNA is converted to nicked circular Form II DNA, which can be further cleaved to form a linear Form III DNA as depicted in Figure 1.22. The three topological forms of DNA may be separated via horizontal agarose gel electrophoresis based upon their different migration rates through the gel. As a result of their different shapes, the compact Form I migrates the fastest; the bulky nicked circular Form II displays a much slower rate compare to Form I; and the linear Form III migrates with a rate intermediate between those of Form I and Form II.

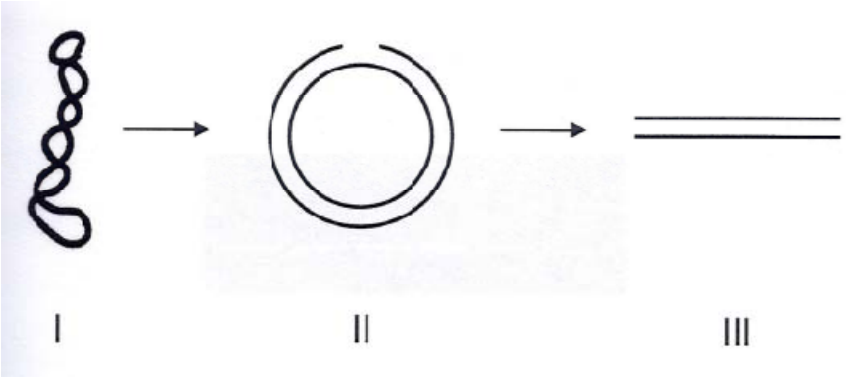

Figure 1.22. Topological forms of plasmid DNA.

1.5 Plan of Study

The research described herein focused on the design, synthesis and study of novel DNA-interactive phenyl benzimidazole–metallopeptide 'hybrids'. In particular, we sought to enhance the DNA binding ability of our original metallopeptides through further modification. In light of the synthesis of benzimidazoles on solid supports,[72] we chose to

modify our basic metallopeptide structure through addition of a phenyl benzimidazole (with or without an amidine end) moiety through solid phase synthesis. In addition, positively charged Lys was used in the Gly_2 position in an effort to maintain a positively-charged metallopeptide domain. As depicted in Figure 1.23, our effort led to three different metallopeptide systems containing phenyl-benzimidazole moieties: (1) a neutral system just like the parent M(II)·Gly-Gly-His metallopeptide; (2) singly positively charged systems with an amidinium group on the benzimidazole moiety or a Lys side chain substitution within the metallopeptide domain; and (3) systems with two positive charges provided by both amidine and Lys side chains. DNA cleavage studies, carried out using these phenyl-benzimidazole modified Gly-Gly-His-derived peptides, revealed that the phenyl-benzimidazole moiety (with or without amidinium groups) led to increased DNA strand scission activity and that Lys substitutions can also facilitate the activity of the whole system.

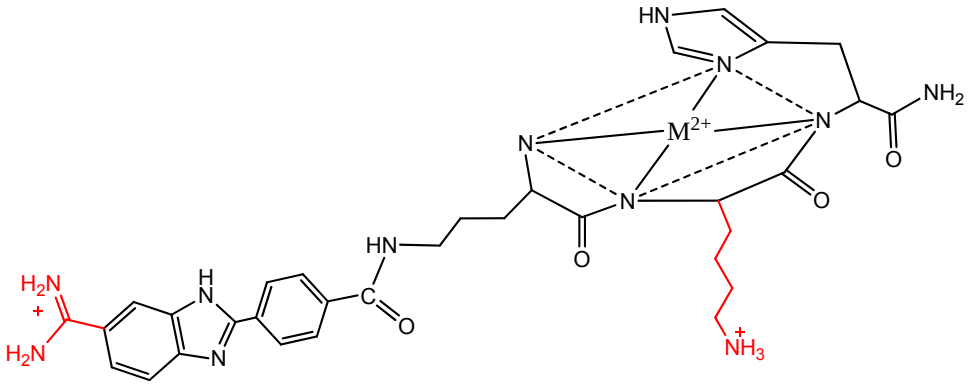

Figure 1.23. Structure of a potential phenyl-benzimidazole modified Gly-Gly-His-derived metallopeptide. Substitutions used are in red.

1.6 List of References

1. Neidle, S. *Nat. Prod. Rep.* **2001**, *18*, 291.

2. Lee, J. S.; Waring, M. J. *Biochem. J.* **1978**, *173*, 115.

3. Tabernero, L.; Verdaguer, N.; Coll, M.; Fita, I.; van der Marel, G. A.; van Boom, J. H.; Rich, A.; Aymami, J. *Biochemistry* **1993**, *32*, 8403.

4. Chen, X.; Ramakrishnan, B.; Sundaralingam, M. *J. Mol. Biol.* **1997**, *267*, 1157.

5. Umezawa, H.; Maeda, K.; Takeuchi, T.; Okami, Y. *J. Antibiot. (Tokyo)* **1966**, *19*, 200.

6. Bremer, R. E.; Baird, E. E.; Dervan, P. B. *Chem. Biol.* **1998**, *5*, 119.

7. Dervan, P. B. *Bioorg. Med. Chem.* **2001**, *9*, 2215.

8. Tanious, F. A.; Laine, W.; Peixoto, P.; Bailly, C.; Goodwin, K. D.; Lewis, M. A.; Long, E. C.; Georgiadis, M. M.; Tidwell, R. R.; Wilson, W. D. *Biochemistry* **2007**, *46*, 6944.

9. Clark, G. R.; Gray, E. J.; Neidle, S.; Li, Y. H.; Leupin, W. *Biochemistry* **1996**, *35*, 13745.

10. Long, E. C. *Accounts Chem. Res.* **1999**, *32*, 827.

11. Shullenberger, D. F.; Eason, P. D.; Long, E. C. *J. Am. Chem. Soc.* **1993**, *115*, 11038.

12. White, E. W.; Tanious, F.; Ismail, M. A.; Reszka, A. P.; Neidle, S.; Boykin, D. W.; Wilson, W. D. *Biophys. Chem.* **2007**, *126*, 140.

13. Le Sann, C.; Baron, A.; Mann, J.; van den Berg, H.; Gunaratnam, M.; Neidle, S. *Org. Biomol. Chem.* **2006**, *4*, 1305.

14. Campbell, N. H.; Evans, D. A.; Lee, M. P.; Parkinson, G. N.; Neidle, S. *Bioorg. Med. Chem. Lett.* **2006**, *16*, 15.

15. Ghosh, A.; Bansal, M. *Acta. Crystallogr. D. Biol. Crystallogr.* **2003**, *59*, 620.

16. Basu, H. S.; Feuerstein, B. G.; Zarling, D. A.; Shafer, R. H.; Marton, L. J. *J. Biomol. Struct. Dyn.* **1988**, *6*, 299.

17. Voet, D., Voet, J. G. *Biochemistry*; 3 ed.; Wiley, **2004.**

18. Marky, L. A.; Breslauer, K. J. *Proc. Natl. Acad. Sci. U. S. A.* **1987**, *84*, 4359.

19. Neto, B. A.; Lapis, A. A. *Molecules* **2009**, *14*, 1725.

20. Huang, X.; Shullenberger, D. F.; Long, E. C. *Biochem. Biophys. Res. Commun.* **1994**, *198*, 712.

21. Lerman, L. S. *J. Mol. Biol.* **1961**, *3*, 18.

22. Boger, D. L.; Tse, W. C. *Bioorg. Med. Chem.* **2001**, *9*, 2511.

23. Tse, W. C.; Boger, D. L. *Acc. Chem. Res.* **2004**, *37*, 61.

24. Waring, M. J. *J. Mol. Biol.* **1965**, *13*, 269.

25. Crawford, L. V.; Waring, M. J. *J. Mol. Biol.* **1967**, *25*, 23.

26. Takenaka, S., Takagi, M. *Bull. Chem. Soc. Jpn.* **1999**, *72*, 327.

27. Geierstanger, B. H.; Wemmer, D. E. *Annu. Rev. Biophys. Biomol. Struct.* **1995**, *24*, 463.

28. Koo, H. S.; Wu, H. M.; Crothers, D. M. *Nature* **1986**, *320*, 501.

29. Finlay, A. C., Hochstein, F. A., Sobin, B. A., Murphy, F. X. *J. Am. Chem. Soc.* **1951**, *73*, 341.

30. Wade, W. S.; Mrksich, M.; Dervan, P. B. *J. Am. Chem. Soc.* **1992**, *114*, 8783.

31. Chen, A. Y.; Yu, C.; Gatto, B.; Liu, L. F. *Proc. Natl. Acad. Sci.* **1993**, *90*, 8131.

32. Abu-Daya, A.; Brown, P. M.; Fox, K. R. *Nucleic. Acids. Res.* **1995**, *23*, 3385.

33. Zimmer, C.; Wahnert, U. *Prog. Biophys. Mol. Biol.* **1986**, *47*, 31.

34. Bailly, C.; Chaires, J. B. *Bioconjug. Chem.* **1998**, *9*, 513.

35. Goodwin, K. D.; Long, E. C.; Georgiadis, M. M. *Nucleic Acids Res.* **2005**, *33*, 4106.

36. Lown, J. W. *J. Mol. Recognit.* **1994**, *7*, 79.

37. Lown, J. W.; Krowicki, K.; Balzarini, J.; De Clercq, E. *J. Med. Chem.* **1986**, *29*, 1210.

38. Walker, W. L.; Kopka, M. L.; Goodsell, D. S. *Biopolymers* **1997**, *44*, 323.

39. Wyatt, M. D.; Garbiras, B. J.; Lee, M.; Forrow, S. M.; Hartley, J. A. *Bioorg.Med. Chem. Lett.* **1994**, *4*, 801.

40. Pelton, J. G.; Wemmer, D. E. *Proc. Natl. Acad. Sci.* **1989**, *86*, 5723.

41. Urbach, A. R.; Love, J. J.; Ross, S. A.; Dervan, P. B. *J. Mol. Biol.* **2002**, *320*, 55.

42. Marques, M. A. D., R. M. Urbach, A. R. and Dervan, P.B. *Helvetica Chimica. Acta.* **2002**, *85*, 4485.

43. Lacy, E. R.; Le, N. M.; Price, C. A.; Lee, M.; Wilson, W. D. *J. Am. Chem. Soc.* **2002**, *124*, 2153.

44. Buchmueller, K. L.; Staples, A. M.; Uthe, P. B.; Howard, C. M.; Pacheco, K. A.; Cox, K. K.; Henry, J. A.; Bailey, S. L.; Horick, S. M.; Nguyen, B.; Wilson, W. D.; Lee, M. *Nucleic Acids Res.* **2005**, *33*, 912.

45. Trauger, J. W.; Baird, E. E.; Dervan, P. B. *J. Am. Chem. Soc.* **1998**, *120*, 3534.

46. Geierstanger, B. H.; Mrksich, M.; Dervan, P. B.; Wemmer, D. E. *Nat. Struct. Biol.* **1996**, *3*, 321.

47. Briehn, C. A.; Weyermann, P.; Dervan, P. B. *Chemistry-a European Journal* **2003**, *9*, 2110.

48. Chenoweth, D. M.; Poposki, J. A.; Marques, M. A.; Dervan, P. B. *Bioorg. & Med. Chem.* **2007**, *15*, 759.

49. Gottesfeld, J. M.; Neely, L.; Trauger, J. W.; Baird, E. E.; Dervan, P. B. *Nature* **1997**, *387*, 202.

50. Nickols, N. G.; Dervan, P. B. *Proc. Natl. Acad. Sci.* **2007**, *104*, 10418.

51. Dervan, P. B.; Doss, R. M.; Marques, M. A. *Curr. Med. Chem. Anticancer Agents* **2005**, *5*, 373.

52. Kraut, E. H., Fleming, T., Segal, M., Neidhart, J. A., Behrens, B. C., MacDonald, J. *Invest. New Drugs* **1991**, *9*, 95.

53. Fede, A.; Labhardt, A.; Bannwarth, W.; Leupin, W. *Biochemistry* **1991**, *30*, 11377.

54. Parkinson, J. A.; Barber, J.; Douglas, K. T.; Rosamond, J.; Sharples, D. *Biochemistry* **1990**, *29*, 10181.

55. Battersby, A. R. *J. Nat. Prod.* **1988**, *51*, 643.

56. Haq, I.; Ladbury, J. E.; Chowdhry, B. Z.; Jenkins, T. C.; Chaires, J. B. *J. Mol. Biol.* **1997**, *271*, 244.

57. Spink, N.; Brown, D. G.; Skelly, J. V.; Neidle, S. *Nucleic Acids Res.* **1994**, *22*, 1607.

58. Clark, G. R.; Boykin, D. W.; Czarny, A.; Neidle, S. *Nucleic Acids Res.* **1997**, *25*, 1510.

59. Ismail, M. A.; Batista-Parra, A.; Miao, Y.; Wilson, W. D.; Wenzler, T.; Brun, R.; Boykin, D. W. *Bioorg. Med. Chem.* **2005**, *13*, 6718.

60. Ismail, M. A.; Brun, R.; Wenzler, T.; Tanious, F. A.; Wilson, W. D.; Boykin, D. W. *Bioorg. Med. Chem.* **2004**, *12*, 5405.

61. Claussen, C. A.; Long, E. C. *Chem. Rev.* **1999**, *99*, 2797.

62. Hecht, S. M.; Long, E.; Heimbrook, D. *Abstracts of Papers of the American Chemical Society* **1986**, *191*, 46.

63. Guajardo, R. J.; Hudson, S. E.; Brown, S. J.; Mascharak, P. K. *J. Am. Chem. Soc.* **1993**, *115*, 7971.

64. Hecht, S. M. *J.Nat. Prod.* **2000**, *63*, 158.

65. Kane, S. A.; Hecht, S. M. *Prog. Nucleic Acid Re.* **1994**, *49*, 313.

66. Hecht, S. M. *Pure. Appl. Chem.* **1989**, *61*, 577.

67. Fang, Y. Y.; Ray, B. D.; Claussen, C. A.; Lipkowitz, K. B.; Long, E. C. *J. Am. Chem. Soc.* **2004**, *126*, 5403.

68. Kimoto, E.; Tanaka, H.; Gyotoku, J.; Morishige, F.; Pauling, L. *Cancer Res.* **1983**, *43*, 824.

69. Liang, Q.; Ananias, D. C.; Long, E. C. *J. Am. Chem. Soc.* **1998**, *120*, 248.

70. Nagane, R.; Koshigoe, T.; Chikira, M.; Long, E. C. *J. Inorg. Biochem.* **2001**, *83*, 17.

71. Claussen, C. A. Ph.D., Purdue University, **2003**.

72. Sun, Q.; Yan, B. *Bioorg. Med. Chem. Lett.* **1998**, *8*, 361.

CHAPTER 2. DESIGN AND SYNTHESIS OF PHENYL-BENZIMIDAZOLE-MODIFIED METALLOPEPTIDES

2.1 Design Considerations

A novel DNA recognition/cleavage system was designed based on the combination of a phenyl-benzimidazole moiety and the DNA cleavage properties of Gly-Gly-His-derived metal binding tripeptides. Given the minor groove targeting of phenyl-benzimidazole and M(II)·Gly-Gly-His derived metallopeptides, it is predicted that these two moieties should act synergistically and lead to increased DNA interaction and enhanced DNA cleavage.

2.1.1 (δ)-Orn-Gly-His Strategy

Although the Gly-Gly-His tripeptide represents a simple yet competent DNA cleavage model, the role played by the terminal amine functionality of this tripeptide unit limits the corporation of this metal binding domain to the amino-terminus of a polypeptide.[1] Several years ago our laboratory developed a method which permits the placement of a Gly_1-Gly_2-His metal binding domain at any location within a linear synthetic peptide chain while preserving its metal-binding, electronic and catalytic properties[2]. The strategy involved introducing an N^{δ}-Fmoc-N^{α}-Boc-ornithine into the amino-terminal Gly_1 position during solid-phase synthesis. This substitution then permits continued synthesis via the deprotected δ-amino group of ornithine.[2] As illustrated in Figure 2.1, the design leaves the α-amino group of Orn free to participate in M(II)

complexation as it would in a tripeptide alone. Given the ability to link the δ amino group of a resin bound Orn to other functionalities[2], we exploited this position for linking and construction of phenyl-benzimidazole moieties with and without additional amidine modifications. Our strategy led to metallopeptide-phenyl-benzimidazole hybrids as shown in Figure 1.23.

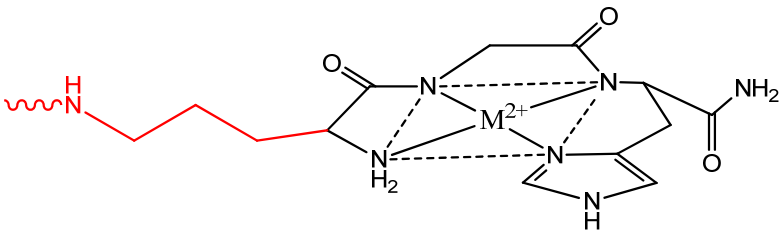

Figure 2.1 The structure of M(II)·(δ)-Orn-Gly-His with the δ-amino group (in red) ready for further coupling.

2.1.2 Amidinium Benzimidazole Solid Phase Synthesis

As mentioned in Chapter 1, several studies have demonstrated that the benzimidazole moiety of some well-documented DNA binding molecules supports an efficient and site-selective DNA association. In addition, aromatic amidines have been prepared as arginine side-chain mimetics due to their favorable electrostatic properties.[3] Thus, as mentioned above, we included amidinium benzimidazole moieties in our design with the aim of obtaining better DNA-interactive systems.

The solution phase synthesis of benzimidazoles has been reported in good yields[4-5] via 1,4-benzoquinone facilitated oxidative coupling of aldehydes with an appropriate 3,4-diaminobenzamidine at high temperature.[6] Recently, a solid-phase synthesis of benzimidazole by making phenylenediamine on Wang resin and then coupling it to soluble imidate was reported.[7] Also, benzimidazoles can be prepared by coupling

4-carboxybenzaldehyde to Wang resin, followed by condensation with phenylenediamines in solution.[8] These reactions can be catalyzed by 1,4 dihydroquinone at elevated temperature (130℃) to drive the reaction to completion.[8]

The introduction of amidinium groups onto benzimidazoles in solution phase synthesis often utilizes substituted aromatic amidines in the coupling step,[9-11] such as the frequently used starting material 3,4-diaminobenzamidine, which can be obtained from the method of Fairley *et al.*[12] An alternatively strategy[6,13] involves the use of the precursor 3,4-diaminobenzonitrile to form a benzimidazole ring, followed by appropriate conversions and reductions. Routes leading to efficient solid phase amidinium benzimidazole synthesis described herein have been explored. Our design involves a combination of several reported approaches.

2.1.3 Amidinium Benzimidazole Tripeptide Conjugates

In light of the (δ)-Orn-Gly-His solid phase synthesis strategy, a series of benzimidazole-tripeptide conjugates were generated. The basic structure of our new design is shown in Figure 2.2.

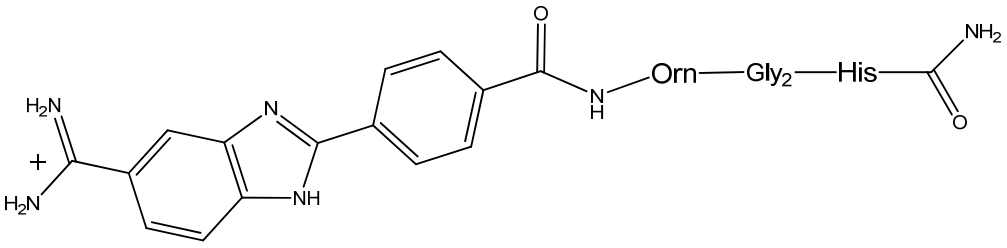

Figure 2.2. Structure of an amidinium-containing benzimidazole-tripeptide conjugate, where Gly_2 can be substituted by Lys.

2.2 Synthesis

A general synthesis scheme leading to our final products is given in Figure 2.3. All syntheses started with Rink amide resin. This resin generates peptides with amide termini upon resin cleavage, thus eliminating the negative charge of a carboxylate; the tripeptides were thus synthesized with C-terminal amides to produce an overall charge neutral complex, and to prevent decarboxylation upon metal binding.[14] Well-established solid-phase peptide synthesis (SPPS) protocols were used to construct the peptide core of the modified conjugates (Figure 2.4). All peptide couplings were confirmed by negative Kaiser tests. Two grams of starting Rink resin was used and split several times to obtain the final products. Peptides **1** and **3** (0.5 g on resin) (Figure 2.3), served as controls and standards for comparison throughout this study. The crude yields obtained were about 95% and the compounds were characterized by LC/MS at $(m+H)^+$: **1** m/z 269, **3** m/z 340 (the predicted m/z are 268.13 and 339.21, respectively). As mentioned before, upon dipeptide synthesis, (δ)-ornithine was then coupled to the solid support to expand the functionalities of the metallopeptides.

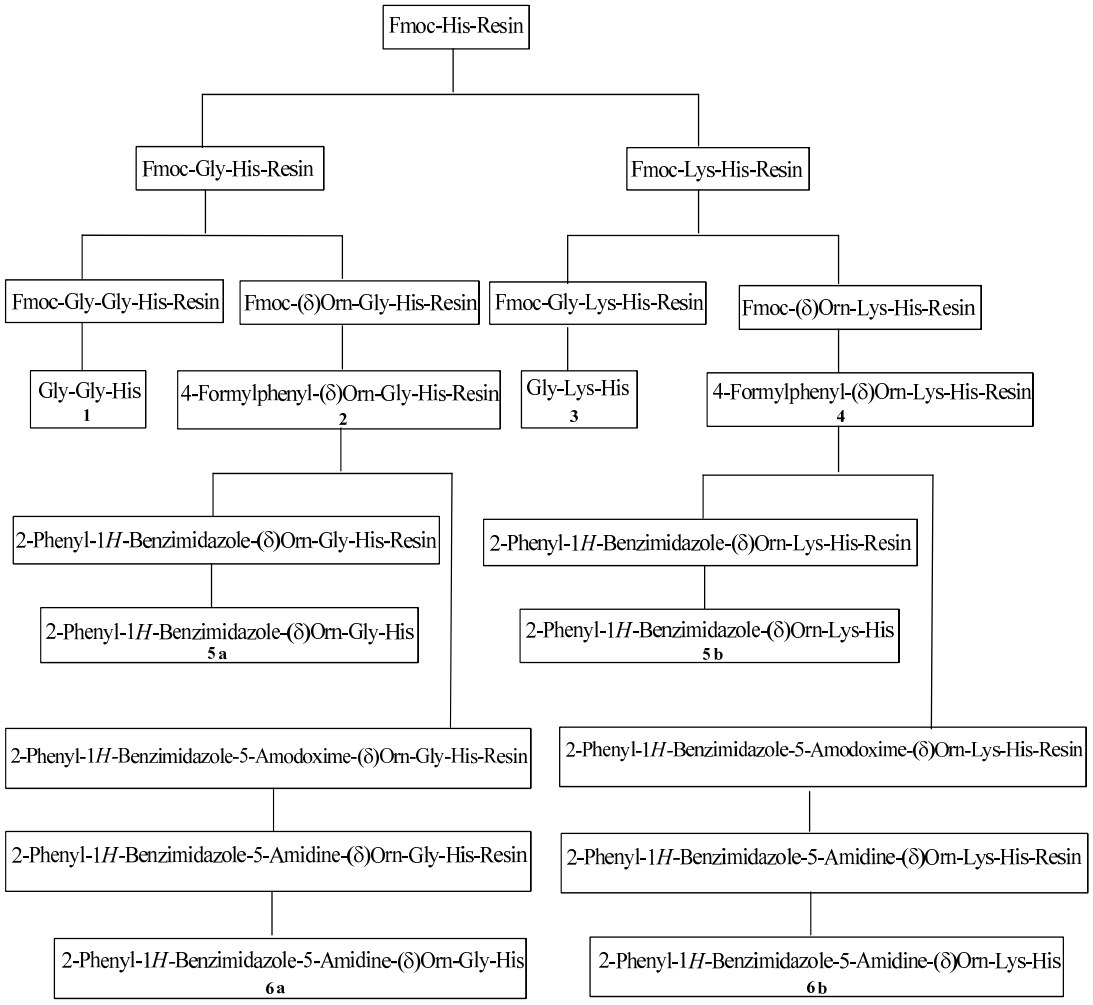

Figure 2.3. Synthetic scheme for the generation of phenyl-benzimidazole modified compounds.

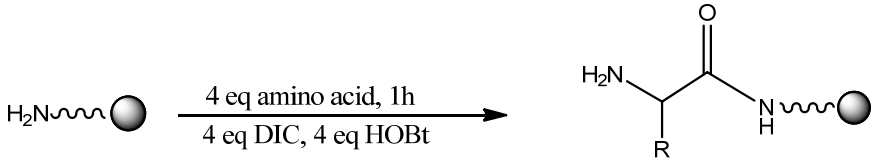

Figure 2.4. Solid-phase amino acid coupling to Rink amide resin.

After coupling all the three amino acids to the resin, 1,4-carboxybenzaldehyde was attached to the δ-amino terminus of ornithine in a similar fashion to obtain compounds **2**

and **4**. Longer reaction times and excess starting materials were used to drive the reaction to complete (Figure 2.5). Resin-bound (δ)-Orn-Gly_2-His was mixed with 5 equiv. starting materials at room temperature with nitrogen bubbling overnight. Completions of couplings were confirmed by negative Kaiser test.

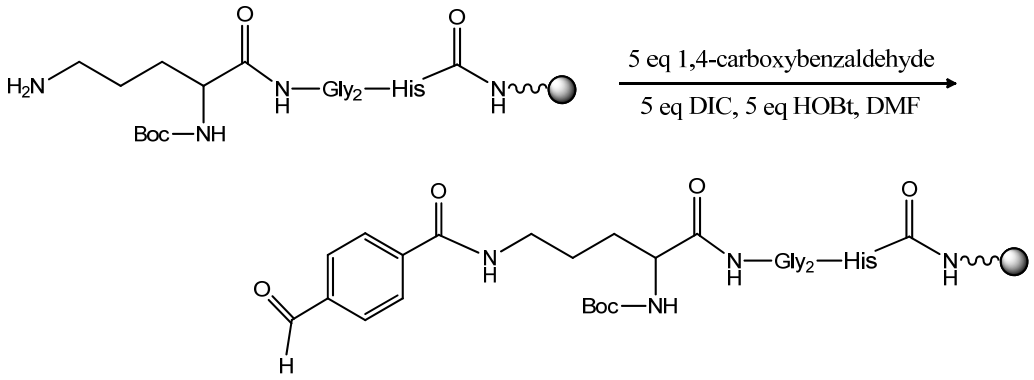

Figure 2.5. Solid-phase coupling of carboxybenzaldehyde to resin-bound (δ)-Orn-Gly_2-His (where Gly_2 can be substituted by Lys).

2.2.1 Compounds without an Amidinium Group (BI-(δ)-Orn-Gly_2-His)

Benzimidazoles have been synthesized in good yields in solution via 1,4-benzoquinone facilitated oxidative coupling of aldehydes with an appropriate 3,4-diaminobenzene at high temperatures.[15] We employed this procedure in our solid-phase synthesis of benzimidazoles. Resin-bound compounds **2** and **4** were each split into two portions. One portion of each resin was then reacted with 10 equiv. of 1,2-diaminobenzene in the presence of 1equiv. of 1,4-benzoquinone. After a reaction time of 5 hours, the products were cleaved from the resin and characterized by LC/MS, $(m+H)^+$: **5a** m/z 546, **5b** m/z 618 (the predicted m/z is 545.25 and 617.33, respectively); $(m+H)^{2+}$: **5a** m/z 273, **5b** m/z 309 (the corresponding predicted m/z are 272.63 and 308.67). The crude yields obtained were approximately 65%.

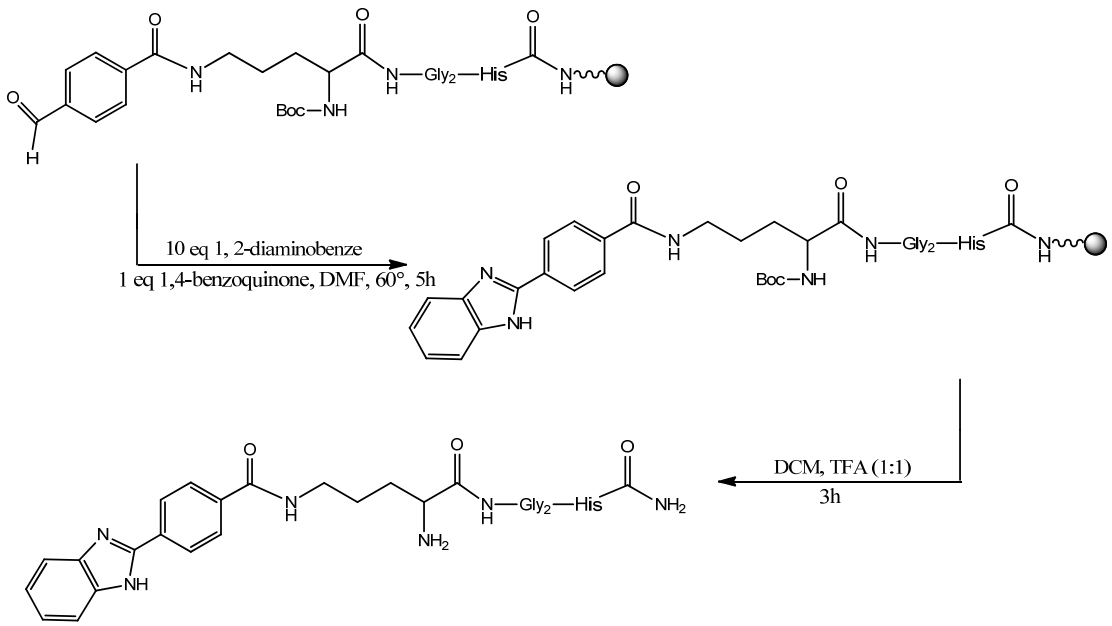

Figure 2.6. Solid-phase synthesis of BI-(δ)-Orn-Gly_2-His, where Gly_2 (**5a**) can be substituted by Lys (**5b**).

2.2.2 Compounds with an Amidinium Group (BI(+)-(δ)-Orn-Gly_2-His)

There are several reported pathways to convert nitriles to amidines, such as the classic/modified Pinner reaction[16-17] and ammonia salts/ammonia conversion (ammonolysis).[18] Unfortunately, applying these strategies to our resin-bound nitriles did not work. In addition to these strategies, Cesar *et al*. developed a new method to synthesize benzamidines on Wang resin. In this case, a benzonitrile was attached to the resin, followed by treatment with hydroxylamine to yield an amidoxime. The final conversion of amidoxime to amidine was realized through reacting the amidoxime with the reducing agent $SnCl_2{\cdot}2H_2O$ (1M solution in DMF).[19] We employed this approach to our tripeptide-amidoxime benizimidazole conjugates. We found that approximately 80% of the benzimidazoles degraded during this step; however, the reduction proceeded well. These results indicated that an alternative strategy was necessary for this conversion.

Towards this end, it has been reported that 3,4-diaminobenzamidines can react with aldehydes to form benzimidazoles under the same conditions as 3,4-diaminobenzonitrile.[20] Given this, our new strategy involved conversion of 3,4-diaminobenzonitrile to the corresponding amidoxime in solution, and then to condense this pre-formed amidoxime with the resin bound aldehyde to form the benzimidazole on solid support. Upon benzimidazole construction, final reduction of the amidoxime moiety by $SnCl_2 \cdot 2H_2O$ can be carried out on the solid support. The preparation of 3,4-diaminobenzamidoxime in solution is shown in Figure 2.7.

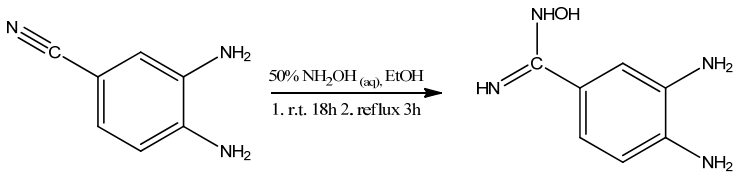

7

Figure 2.7. The preparation of 3,4-diaminobenzamidoxime (**7**) in solution.

The other two resin portions split from compounds **2** and **4** were used to couple with 3,4-diaminobenzamidoxime in the above-described way. This reaction was monitored by cleaving a small amount of resin and conducting LC/MS characterization of the intermediate benzamidoxime. Further reduction of the resulting amidoximes were performed by adding 15 equiv. of $SnCl_2 \cdot 2H_2O$ (1M solution in DMF) to the reaction vials. The reaction proceeded under argon at 80℃ for 40h to allow the complete conversion (Figure 2.8).[19] All products were cleaved from resin under standard conditions. Amidine conjugates were characterized by LC/MS at $(m+H)^+$: **6a** m/z 588, **6b** m/z 659 (the predicted m/z are 587.28 and 658.36, respectively); $(m+H)^{2+}$: **6a** m/z 294, **6b** m/z 330 (the

corresponding predicted m/z are 293.64 and 329.18). The crude yields obtained were 50%.

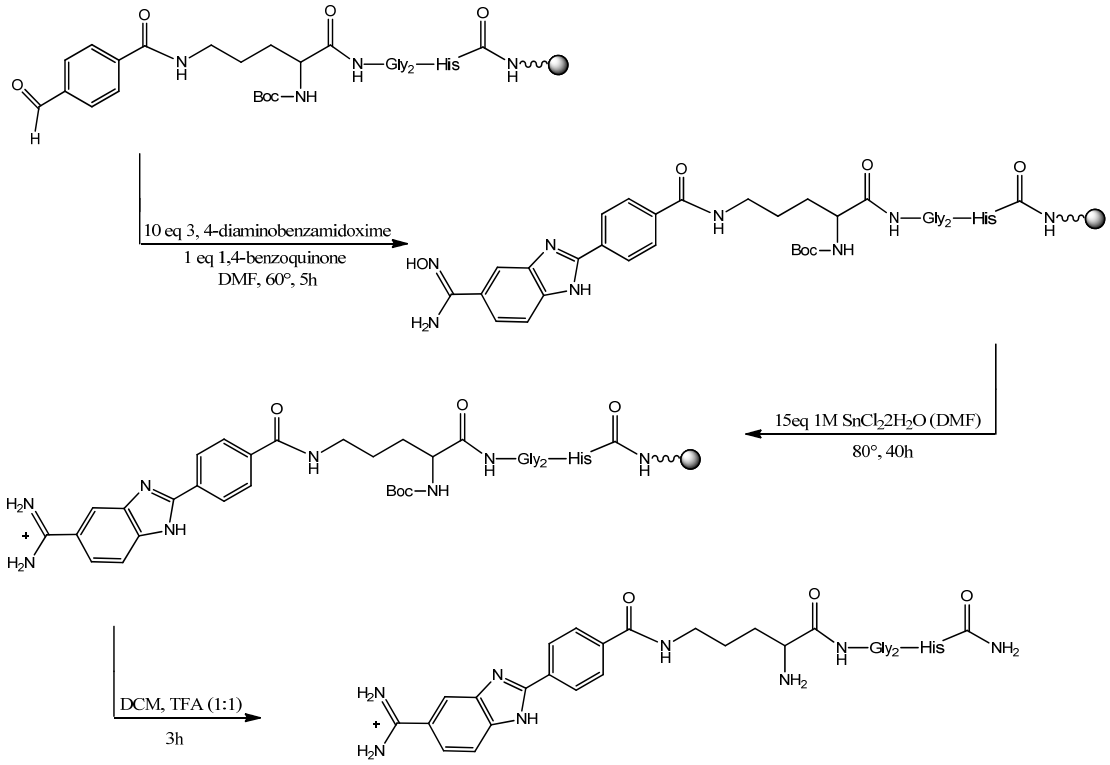

Figure 2.8. Solid-phase synthesis of Bl(+)-(δ)-Orn-Gly_2-His (where Gly_2 (**6a**) can be substituted by Lys (**6b**)).

2.3 Summary of Synthesis

An efficient solid-phase synthesis protocol to generate phenyl-benzimidazole tripeptide conjugates was developed. The amino acids were coupled to Rink resins using standard protocols, followed by attachment to carboxybenzaldehyde under similar conditions. The resultant resin bound benzaldehydes were then mixed with pre-synthesized diaminobenzamidoximes, catalyzed by 1,4-benzoquinone, to form benzimidazole rings. The final step involved the reduction of resin-bound amidoxime by tin chloride. After resin cleavage and appropriate purification procedures, all the products were characterized by LC/MS.

2.4 Experimental Protocols

2.4.1 General Considerations

Solid phase syntheses were carried out in glass reactors with sintered frits or glass vials. Commercially available Fmoc-protected amino acids and 4-(2',4'-dimethoxyphenyl-Fmoc-aminomethyl)-phenoxymethyl-polystyrene resins (Rink resin; 200-400 mesh) were purchased from Biochem and EMD. Other chemicals and solvents were reagent grade or better and were obtained from Sigma-Aldrich, Fisher Scientific, or other commercial sources.

Silica gel chromatography was performed using a self-packed columns. Preparative HPLC purifications were carried out on a Varian 2200 series HPLC equipped with a C-18 semi preparative column. Mass spectra were determined on an Ailgent 1100 series LC/MS.

2.4.2 Synthesis

2.4.2.1 Solid-Phase Peptide Synthesis

Tripeptide cores were synthesized using standard solid-phase Fmoc protocols. 2 g of resin was first allowed to swell in dichloromethane (DCM) for approximately 30 min. After rinsing this resin six times with *N*,*N*-dimethylformamide (DMF), the Fmoc protecting group was removed from the resin by mixing with a 30% piperidine/70% DMF solution for 15 min. The resin was then rinsed alternatively with DMF and isopropanol (IPA). A Kaiser test was preformed to verify amine deprotection. In a separate Erlenmeyer flask, a 4-fold molar excess of Fmoc-protected amino acid, diisopropylcarbodiimide (DIC) and 1-hydroxybenzotriazole (HOBt) was dissolved in DMF and then added to the resin and

mixed for approximately 1h. Following amino acid coupling, the resin was rinsed with DMF/IPA. A second Kaiser test was then performed to verify the presence of protected terminal amine, and thus successful coupling. Additional amino acids were added by repeating this procedure, beginning with Fmoc deprotection of the resin bound starting material. For peptide syntheses in this study, 2 g of resin was split into four portions, peptides **1** and **3** were cleaved off the resin by mixing with TFA and CH_2Cl_2 (1:1) solution for 3 h, after which the peptides were precipitated from cold methyl-*tert* butyl ether (MTBE). Centrifugation and lyophylization were then employed to concentrate and dry the crude peptide products.

2.4.2.2 1,4-Carboxybenzaldehyde Coupling

The remaining two portions of resin split from the original 2 g (see above) of starting resin Fmoc-(δ)-Orn-Gly/Lys-His (0.5 g) were used continued to couple with 1,4-carboxybenzaldehyde after the deprotection of the δ-amine of ornithine. 5-fold molar excesses of 1,4-carboxybenzaldehyde (0.23 g) were mixed and activated with DIC (235 μL), HOBt (0.2 g) and DIPEA (105 μL). The mixture was then added to the reactor vessel and bubbled with N_2 overnight. The products **5a** and **5b** were rinsed with DMF/IPA and a Kaiser test was performed to assure the completion of the reaction.

2.4.2.3 3,4-Diaminobenzamidoxime

3,4-diaminobenzonitrile (2.4 mmol, 0.32 g) was dissolved in absolute EtOH (30 ml) and excess 50% aqueous hydroxylamine (1.0 ml) was added. The mixture was stirred for 18h at room temperature, followed by refluxing for 3h and cooling to room temperature. Upon concentration under reduced pressure, silica gel (2 g) was added to form a powder for purification. The crude silica-bound product was loaded on a packed flash column and eluted with EtOAc/MeOH. Fractions were collected with 1-10% MeOH in EtOAc to give

7. The product was confirmed by LC/MS: $(M+H)^+$ m/z 167 (the predicted m/z is 166.09) and the yield is approximately 95%.

2.4.2.4 On-resin Benzimidazole Ring Construction

Resin bound compounds **2** and **4** were split into two portions and mixed with pre-dissolved 3,4-diaminobenzene (10 equiv.) and 1, 4-benzoquinone (1 equiv.); 3,4-diaminobenzamidoxime (compound **13**) and 1,4-benzoquinone of the same ratio, respectively. The mixtures were heated to 60℃ and stirred for 16h in glass vials. The Products **5a** and **6a** were cleaved from the resin with TFA/CH_2Cl_2 (1:1). The brownish compounds were subjected to centrifugation, lyophylization and purification. The crude yields were approximately 65%.

2.4.2.5 Amidoxime Reduction

Resin bound amidoximes were transferred to glass vials and mixed with 15 equiv. of $SnCl_2$ (1 M solution in DMF). The reaction was conducted at 80℃ under argon for 40 h. Products were rinsed with DMF/IPA and cleaved from the resins under standard conditions. The same purification procedure as described in section 2.4.4 was employed to obtain **5b** and **6b**. The crude yields were approximately 50%.

2.4.3 Purification

C18 reversed-phase HPLC purification was performed for all products (BI-(δ)-Orn-Gly-His, BI-(δ)-Orn-Lys-His, BI(+)-(δ)-Orn-Gly-His, and BI(+)-(δ)-Orn-Lys-His). Conditions are listed as follow: Solvent A: H_2O with 0.1% TFA, Solvent B: ACN with 0.1% TFA. Gradient: 0 min 95% A; 2 min 75% A; 5 min 60% A; 15 min 50% A; 17 min 100% B; 19 min 95% A.

2.5 List of References

1. Long, E. C. E., P. D.; Liang, Q. *Met. Ions Biol. Syst.* **1996**, *33*, 427.

2. Shullenberger, D. F.; Eason, P. D.; Long, E. C. *J.Am. Chem. Soc.* **1993**, *115*, 11038.

3. Zablocki, J. A.; Miyano, M.; Garland, R. B.; Pireh, D.; Schretzman, L.; Rao, S. N.; Lindmark, R. J.; Panzer-Knodle, S. G.; Nicholson, N. S.; Taite, B. B.; et al. *J. Med. Chem.* **1993**, *36*, 1811.

4. Bathini, Y. L., J. W. *Synth. Commun.* **1991**, *21*, 215

5. Singh, M. P.; Joseph, T.; Kumar, S.; Bathini, Y.; Lown, J. W. *Chem. Res. Toxicol.* **1992**, *5*, 597.

6. Wendt, M. D.; Rockway, T. W.; Geyer, A.; McClellan, W.; Weitzberg, M.; Zhao, X.; Mantei, R.; Nienaber, V. L.; Stewart, K.; Klinghofer, V.; Giranda, V. L. *J. Med. Chem.* **2004**, *47*, 303.

7. Phillips, G. B.; Wei, G. P. *Tetrahedron Lett.* **1996**, *37*, 4887.

8. Sun, Q.; Yan, B. *Bioorg. Med. Chem. Lett.* **1998**, *8*, 361.

9. Mackman, R. L.; Hui, H. C.; Breitenbucher, J. G.; Katz, B. A.; Luong, C.; Martelli, A.; McGee, D.; Radika, K.; Sendzik, M.; Spencer, J. R.; Sprengeler, P. A.; Tario, J.; Verner, E.; Wang, J. *Bioorg. Med. Chem. Lett.* **2002**, *12*, 2019.

10. Shrader, W. D.; Kolesnikov, A.; Burgess-Henry, J.; Rai, R.; Hendrix, J.; Hu, H.; Torkelson, S.; Ton, T.; Young, W. B.; Katz, B. A.; Yu, C.; Tang, J.; Cabuslay, R.; Sanford, E.; Janc, J. W.; Sprengeler, P. A. *Bioorg. Med. Chem. Lett.* **2006**, *16*, 1596.

11. Vijaykumar, D.; Sprengeler, P. A.; Shaghafi, M.; Spencer, J. R.; Katz, B. A.; Yu, C.; Rai, R.; Young, W. B.; Schultz, B.; Janc, J. *Bioorg. Med. Chem. Lett.* **2006**, *16*, 2796.

12. Fairley, T. A.; Tidwell, R. R.; Donkor, I.; Naiman, N. A.; Ohemeng, K. A.; Lombardy, R. J.; Bentley, J. A.; Cory, M. *J. Med. Chem.* **1993**, *36*, 1746.

13. Ismail, M. A.; Brun, R.; Wenzler, T.; Tanious, F. A.; Wilson, W. D.; Boykin, D. W. *Bioorgan. Med. Chem.* **2004**, *12*, 5405.

14. Bal, W. D., M. I.; Margerum, D. W.; Gray Jr., E. T. ; Mazid, M. A.; Tom, R. T.; Nieboer, E.; Sadler, P. J. *J. Chem. Soc., Chem. Commun.* **1993**, 1889.

15. Kang, Z.; Dykstra, C. C.; Boykin, D. W. *Molecules* **2004**, *9*, 158.

16. Goker, H.; Ozden, S.; Yildiz, S.; Boykin, D. W. *Eur. J. Med. Chem.* **2005**, *40*, 1062.

17. Lange, U. E. W. S., B.*; Baucke, D.; Buschmann, E.; Mack, H. *Tetrahedron Lett.* **1999**, *40*, 7067.

18. SCHAEFER, F. C. *J. Org. Chem.* **1962**, *27*, 3608.

19. Cesar, J.; Nadrah, K.; Dolenc, M. S. *Tetrahedron Lett.* **2004**, *45*, 7445.

20. Verner, E.; Katz, B. A.; Spencer, J. R.; Allen, D.; Hataye, J.; Hruzewicz, W.; Hui, H. C.; Kolesnikov, A.; Li, Y.; Luong, C.; Martelli, A.; Radika, K.; Rai, R.; She, M.; Shrader, W.; Sprengeler, P. A.; Trapp, S.; Wang, J.; Young, W. B.; Mackman, R. L. *J. Med. Chem.* **2001**, *44*, 2753.

CHAPTER 3. DNA CLEAVAGE ACTIVITY OF PHENYL-BENZIMIDAZOLE MODIFIED GLY-GLY-HIS-DERIVED METALLOPEPTIDES

3.1 Overview

Our design envisioned that the benzimidazole modified Gly-Gly-His-derived systems should exhibit increased DNA cleavage activity due to the presence of the benzimidazole moiety. Previous work[1] indicated that the (δ)-Orn-Gly-His systems bind metals in a fashion identical to Gly-Gly-His system. In the present case, tripeptides with the phenyl-benzimidazole (+/-) functionalities may bind to metal slightly differently, but it is reasonable to assume that the tetradentate metal binding capabilities of the peptide should dominate metal binding. This investigation thus sought to determine if the phenyl-benzimidazole moieties (with or without amidines) attached to the metal binding domain influences metallopeptide-DNA interactions. Moreover, previous studies have found that Lys or Arg substituted Ni(II)·Gly_1-Gly_2-His metallopeptides possess enhanced levels of DNA cleavage activity relative to Ni(II)·Gly-Gly-His, therefore, the influence of Lys substitutions within the modified tripeptides was also examined. Thus, as listed in Figure 3.1, two groups of peptides were investigated based on the amino acid present at the Gly_2 position: (1) Gly-Gly-His and its derivatives in contrast to (2) Gly-Lys-His and its derivatives.

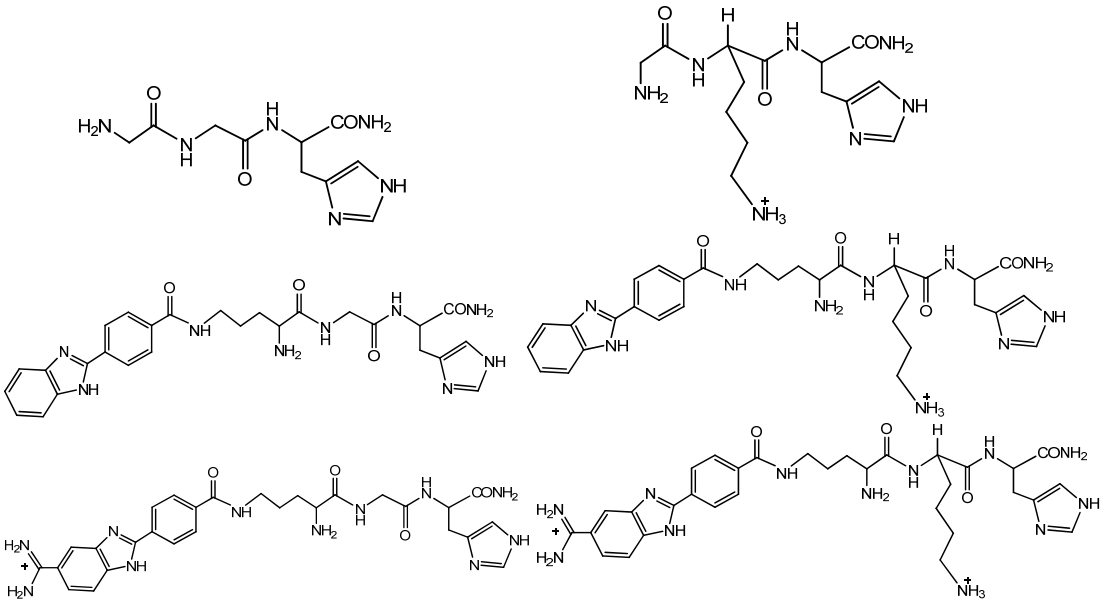

A B

Figure 3.1. Structures of all compounds employed in DNA cleavage studies. Gly-Gly-His and its derivatives (A); Gly-Lys-His and its derivatives (B).

3.2 Results and Discussion

The ability of Ni(II)·Gly-Gly$_2$-His (where Gly$_2$ may be substituted by Lys) to mediate the conversion of supercoiled (form I) DNA to nicked circular (form II) DNA was assessed via the plasmid DNA cleavage assay discussed in Chapter 1.

3.2.1 DNA Cleavage by Ni(II)·Gly-Gly-His and its Derivatives (**1, 5a, 6a**)

To determine the effect of benzimidazoles (+/-) on the DNA cleavage activities of these systems, a comparison to Gly-Gly-His alone was carried out. The results from this side-by-side analysis are shown in Figure 3.2 with lanes 1-5 employed as controls, lanes 6-8, lanes 9-11, and lanes 12-14 served as DNA cleavage reaction with Gly-Gly-His (**1**), BI-(δ)-Orn-Gly-His (**5a**) and BI(+)-(δ)-Orn-Gly-His (**6a**), respectively. As expected, given their structures, phenyl-benzimidazole modified Gly-Gly-His-derived compounds exhibited much greater DNA cleavage reactivity than the standard tripeptide Gly-Gly-His

alone. In particular, the amidinium derivative displayed an enhanced DNA cleavage ability with more pronounced bands of form II DNA (lane 12, 13, and 14). Therefore, the DNA strand scission efficiencies of the ligands in this series were determined to be: Ni(II)·BI(+)-(δ)Orn-Gly-His (**6a**) > Ni(II)·BI-(δ)Orn-Gly-His (**5a**) > Ni(II)·Gly-Gly-His (**1**).

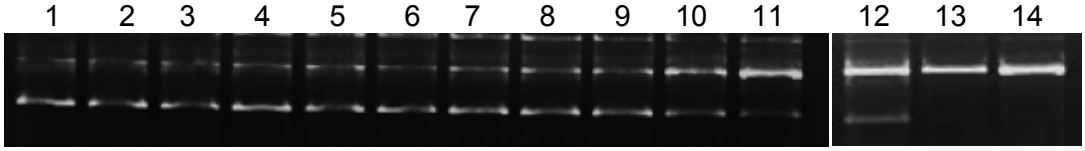

Figure 3.2. Agarose gel analysis of Ni(II)·Gly-Gly-His, Ni(II)·BI-(δ)-Orn-Gly-His and Ni(II)·BI(+)-(δ)-Orn-Gly-His induced cleavage of supercoiled ***ΦX***174RF plasmid DNA. All reactions contained 30 μM DNA bp and 10mM sodium cacodylate buffer, PH 7.4. Lane 1, reaction control (DNA); lane 2, reaction control (DNA, 10 μM $Ni^{2+,}$ 10 μM $KHSO_5$); lane 3, reaction control (DNA, 10 μM $KHSO_5$, 12 μM GGH); lane 4, reaction control (DNA, 10 μM $KHSO_5$, 12 μM BI-(δ)OGH); lane 5, reaction control (DNA, 10 μM $KHSO_5$, 12 μM BI(+)-(δ)OGH); lane 6 (2.5 μM Ni^{2+}, 2.5 μM $KHSO_5$, 3 μM GGH); lane 7 (5 μM Ni^{2+}, 5 μM $KHSO_5$, 6 μM GGH); lane 8 (10 μM Ni^{2+}, 10 μM $KHSO_5$,12 μM GGH); lane 9 (2.5 μM Ni^{2+}, 2.5 μM $KHSO_5$, 3 μM BI-(δ)OGH); lane 10 (5 μM Ni^{2+}, 5 μM $KHSO_5$, 6 μM BI-(δ)OGH); lane 11 (10 μM Ni^{2+}, 10 μM $KHSO_5$, 12 μM BI-(δ)OGH); lane 12 (2.5 μM Ni^{2+}, 2.5 μM $KHSO_5$, 2.5 μM BI(+)-(δ)OGH); lane 13 (5 μM Ni^{2+}, 5 μM $KHSO_5$, 6 μM BI(+)-(δ)OGH); lane 14 (10 μM Ni^{2+}, 10 μM $KHSO_5$, 12 μM BI(+)-(δ)OGH).

The improved activity of Gly-Gly-His modified ligands may be attributed to three factors. First, the phenyl-benzimidazole group (with or without amidines) is the building block of many well-known DNA minor groove binders. The well-studied compound Hoechst 33258, which is mainly made up of two benzimidazole incorporated units in a head-to-tail manner. The X-ray crystallographic and NMR studies on complexes of Hoechst 33258 with A·T-containing oligonucleotides have shown that the ligand is bound in the minor groove, with the planar benzimidazole groups oriented parallel to the groove with each inner-facing nitrogen atom hydrogen bonding in a bifurcated manner to a pair of adjacent hydrogen-bond donors on the edge of the A·T base pairs.[2] Thermodynamically speaking, the additional hydrogen bonding driving force may lead to stronger equilibrium binding to DNA. The incorporation of the flat benzimidazole group also provides more

points of contact within the minor groove floor of A·T rich region and leads to more favorable van der Waals interactions between DNA and the ligands. Studies found that the benzimidazole-derived compound showed an induced fit structure change to place functional groups in position to interact with bases at the floor of the groove.[3-4] This 'flexibility' feature makes benzimidazole moiety a very powerful tool which likely is working synergistically with our peptide complexation toward DNA binding and function to accelerate DNA cleavage.

Second, the tethering of a phenyl-benzimidazole functional group to a metallopeptide may further stabilize the reactive complex formed via $KHSO_5$. Previous M(II)·Xaa_1-Xaa_2-His metallopeptide-DNA cleavage studies have proposed that the active species responsible for deoxyribose damage is a peptide-bound Ni (III)-HO· or Ni(IV)=O, which is generated through the heterolytic splitting of the oxygen-oxygen bond present in $KHSO_5$.[5] The π system of the conjugated aromatic rings is able to delocalize electrons and help facilitate the stabilization of reactive high-valent metal ions, thus perhaps enhancing the rate of DNA cleavage relative to Ni(II)·Gly-Gly-His (**1**).

Third, electrostatic interactions are likely to play an important role in the increased reactivity of Ni(II)·BI(+)-(δ)Orn-Gly-His (**5b**) vs. tripeptides alone. A net positive charge makes the complex more attractive to the polyanionic DNA helix and the increased local concentration of ligands in proximity to DNA allow the system to act more efficiently. Additionally, the amidine moiety is an important pharmacophore group in biologically active agents which is correlated with its ability to interact strongly with the DNA minor groove in A·T sequences.[6] Therefore, the incorporated amidine group provides added stability to the bound complex.

3.2.2 DNA Cleavage by Ni(II)·Gly-Lys-His and its Derivatives (**3, 5b, 6b**)

The affect of Lys substitution at the second position within the tripeptide ligand was examined also. Previous studies[7-8] of unmodified tripeptides have confirmed that Lys substitutions lead to enhanced cleavage efficiency, likely due to the increased positive charge density on the peptide and the ability of Lys residue to stabilize the metal-peptide complexes.[7] A comparison between Ni(II)·Gly-Gly-His (**1**) and Ni(II)·Gly-Lys-His (**3**) shown in Figure 3.3 supports this point of view.

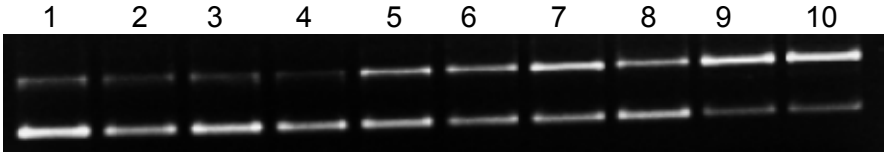

Figure 3.3. Agarose gel analysis of Ni(II)·Gly-Gly-His and Ni(II)·Gly-Lys-His induced cleavage of supercoiled ***ΦX***174RF plasmid DNA. All reactions contained 30 μM DNA bp and 10mM sodium cacodylate buffer, PH 7.4. lane 1, reaction control (DNA); lane 2, reaction control (DNA, 300 μM $Ni^{2+,}$ 300μM $KHSO_5$); lane 3, reaction control (DNA, 300 μM $KHSO_5$, 360 μM GGH); lane 4, reaction control (DNA, 300 μM $KHSO_5$, 360 μM GKH); lane 5 (100 μM Ni^{2+}, 100 μM $KHSO_5$, 120 μM GGH); lane 6 (200 μM Ni^{2+}, 200 μM $KHSO_5$, 240 μM GGH); lane 7 (300 μM Ni^{2+}, 300 μM $KHSO_5$,360 μM GGH); lane 8 (100 μM Ni^{2+}, 100 μM $KHSO_5$, 120 μM GKH); lane 9 (200 μM Ni^{2+}, 200 μM $KHSO_5$, 240 μM GKH); lane 10 (300 μM Ni^{2+}, 300 μM $KHSO_5$, 360 μM GKH).

Similarly, the attachment of a phenyl-benzimidazole group to the GKH ((δ)-OKH) tripeptide promoted DNA strand scission. With regard to the ligand containing an amidine group, interestingly, as illustrated in Figure 3.4, it appears that Ni(II)·BI(+)-(δ)Orn-Lys-His (**6b**) maintained a cleavage activity similar to that of Ni(II)·BI-(δ)Orn-Lys-His (**5b**). Compared to Ni(II)·BI-(δ)Orn-Lys-His (**6a**) which bears one positive charge, Ni(II)·BI(+)-(δ)Orn-Lys-His (**6b**) metallopeptide carries two positive charges. This observation implies that the addition of a Lys residue to the modified system is no longer a simple additive effect with regard to electrostatic forces. To further analyze the factors

that could potentially influence the reactivity of these ligands, a comparative experiment between the two groups was performed.

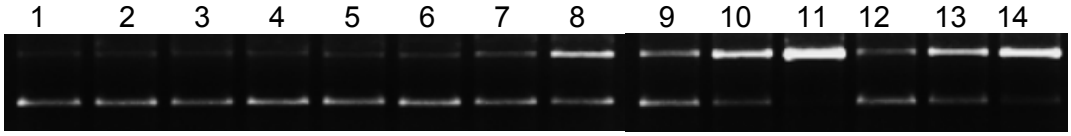

Figure 3.4. Agarose gel analysis of Ni(II)·Gly-Lys-His, Ni(II)·BI-(δ)-Orn-Lys-His and Ni(II)·BI(+)-(δ)-Orn-Lys-His induced cleavage of supercoiled $\boldsymbol{\Phi X}$174RF plasmid DNA. All reactions contained 30 μM DNA bp and 10mM sodium cacodylate buffer, PH 7.4. Lane 1, reaction control (DNA); lane 2, reaction control (DNA, 10 μM $Ni^{2+,}$ 10 μM $KHSO_5$); lane 3, reaction control (DNA, 10 μM $KHSO_5$, 12 μM GKH); lane 4, reaction control (DNA, 10 μM $KHSO_5$, 12 μM BI-(δ)OKH); lane 5, reaction control (DNA, 10 μM $KHSO_5$, 12 μM BI(+)-(δ)OKH); lane 6 (2.5 μM Ni^{2+}, 2.5 μM $KHSO_5$, 3 μM GKH); lane 7 (5 μM Ni^{2+}, 5 μM $KHSO_5$, 6 μM GKH); lane 8 (10 μM Ni^{2+}, 10 μM $KHSO_5$,12 μM GKH); lane 9 (2.5 μM Ni^{2+}, 2.5 μM $KHSO_5$, 3 μM BI-(δ)OKH); lane 10 (5 μM Ni^{2+}, 5 μM $KHSO_5$, 6 μM BI-(δ)OKH); lane 11 (10 μM Ni^{2+}, 10 μM $KHSO_5$, 12 μM BI-(δ)OKH); lane 12 (2.5 μM Ni^{2+}, 2.5 μM $KHSO_5$, 2.5 μM BI(+)-(δ)OKH); lane 13 (5 μM Ni^{2+}, 5 μM $KHSO_5$, 6 μM BI(+)-(δ)OKH); lane 14 (10 μM Ni^{2+}, 10 μM $KHSO_5$, 12 μM BI(+)-(δ)OKH).

As shown in Figure 3.5, Ni(II)·BI(+)-(δ)-Orn-Gly-His (**5b**) metallopeptide cleaved DNA to a much greater extent than Ni(II)·BI-(δ)-Orn-Gly-His (**5a**), Ni(II)·BI-(δ)-Orn-Lys-His (**6a**) and Ni(II)·BI(+)-(δ)-Orn-Lys-His (**6b**). The results suggest that the incorporation of an amidinium benzimidazole terminus optimizes the metallopeptide-DNA interaction as compared to the α-carbon substituent within the peptides resulting in increased DNA cleavage activity. With regard to Ni(II)·BI(+)-(δ)-Orn-Lys-His (**6b**) which is equipped with both a terminal amidine and an α-carbon Lys substituent, perhaps the coexistence of them decreases the flexibility of the complex and results in conformations with less favorable metallopeptide-DNA orientations. The result also indicates that the inclusion of a Lys residue at the second position within the modified ligand (Ni(II)·BI-(δ)-Orn-Lys-His) enhances DNA cleavage reactivity relative to the Ni(II)·BI-(δ)-Orn-Gly-His (**5a**) metallopeptide.

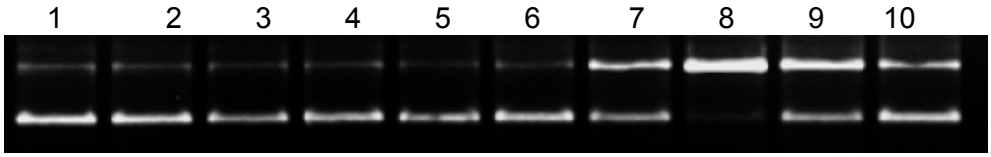

Figure 3.5. Agarose gel analysis of Ni(II)·BI-(δ)-Orn-Gly-His, Ni(II)·BI(+)-(δ)-Orn-Gly-His, Ni(II)·BI-(δ)-Orn-Lys-His and Ni(II)·BI(+)-(δ)-Orn-Lys-His induced cleavage of supercoiled ***ΦX***174RF plasmid DNA. All reactions contained 30 μM DNA bp and 10mM sodium cacodylate buffer, PH 7.4. lane 1, reaction control (DNA); lane 2, reaction control (DNA, 5 μM Ni^{2+}, 5 μM $KHSO_5$); lane 3, reaction control (DNA, 5 μM $KHSO_5$, 6 μM BI-(δ)OGH); lane 4, reaction control (DNA, 5 μM $KHSO_5$, 6 μM BI(+)-(δ)OGH); lane 5, reaction control (DNA, 5 μM $KHSO_5$, 6 μM BI-(δ)OKH); lane 6 reaction control (DNA, 5 μM $KHSO_5$, 6 μM BI(+)-(δ)OKH); lane 7 (5 μM Ni^{2+}, 5 μM $KHSO_5$, 6 μM BI-(δ)OGH); lane 8 (5 μM Ni^{2+}, 5 μM $KHSO_5$, 6 μM BI(+)-(δ)OGH); lane 9 (5 μM Ni^{2+}, 5 μM $KHSO_5$, 6 μM BI-(δ)OKH); lane 10 (5 μM Ni^{2+}, 5 μM $KHSO_5$, 6 μM BI(+)-(δ)OKH).

3.3 Conclusions

The DNA cleavage studies described in this chapter demonstrated that (1) tripeptides with phenyl-benzimidazole functionalities have enhaced DNA cleavage and (2) the phenyl-benzimidazole-modified Gly-Gly-His-derived metallopeptides exhibited an increased DNA strand scission efficiency relative to the standard Ni(II)·Gly-Gly-His metallopeptide. In addition, a side by side comparison of Ni(II)·BI-(δ)Orn-Gly-His, Ni(II)·BI(+)-(δ)Orn-Gly-His, Ni(II)·BI-(δ)Orn-Lys-His, and Ni(II)·BI(+)-(δ)Orn-Lys-His revealed that the amidinium benzimidazole moiety contributes to DNA cleavage activity. However, more techniques, such as FID (fluorescence intercalator displacement) and molecular dynamic simulations need to be employed to thoroughly elucidate the DNA binding modes and site selectivities of these ligands.

The development of N-terminal modified metallopeptides could further our understanding of protein- and small molecule-DNA interactions and assist in the redesign of naturally-occurring antitumor agents. Using these methods, other documented DNA recognition moieties in addition to benzimidazole could be employed to impart enhanced DNA site selectivity to the metallopeptides. Meanwhile, the utilization of other amino

acids within the peptide portion may increase the reactivity of the complexes. For example, Met, Ser and Thr in the Gly_2 position proved to result in increased DNA cleavage activity.[9] In fact, it may be possible in the future to build a combinatorial library of these systems by tuning the intrinsic properties of these modified metallopeptides.

3.4 Experimental Protocols

DNA cleavage reactions were prepared by first pre-incubating modified peptides with $Ni(OAc)_2$ at a ratio of metal to metal binding site of 1:1.2 in 10 mM sodium cacodylate buffer (pH 7.4) to form the metallopeptide complex. This was followed by the addition of ***Φ***X174 RF DNA (30 μM base pair final concentration). After incubating the reaction mixtures for 10 min at room temperature, cleavage reactions were initiated upon the addition of $KHSO_5$ in an amount equimolar to Ni(II) and quenched after one minute by adding an EDTA containing loading buffer. Reaction aliquots were loaded onto 0.9% agarose gels containing 5 μg/ml ethidium bromide and electrophoresed in TAE buffer at 60 volts for 2 h and visualized using a UV transilluminator.

3.5 List of References

1. Shullenberger, D. F.; Eason, P. D.; Long, E. C. *J.Am. Chem. Soc.* **1993**, *115*, 11038.

2. Neidle, S. *Nat. Prod. Rep.* **2001**, *18*, 291.

3. Miao, Y.; Lee, M. P.; Parkinson, G. N.; Batista-Parra, A.; Ismail, M. A.; Neidle, S.; Boykin, D. W.; Wilson, W. D. *Biochemistry* **2005**, *44*, 14701.

4. Tanious, F. A.; Laine, W.; Peixoto, P.; Bailly, C.; Goodwin, K. D.; Lewis, M. A.; Long, E. C.; Georgiadis, M. M.; Tidwell, R. R.; Wilson, W. D. *Biochemistry* **2007**, *46*, 6944.

5. Long, E. C. *Accounts Chem. Res.* **1999**, *32*, 827.

6. Chaires, J. B.; Ren, J.; Hamelberg, D.; Kumar, A.; Pandya, V.; Boykin, D. W.; Wilson, W. D. *J. Med. Chem.* **2004**, *47*, 5729.

7. Jin, Y.; Lewis, M. A.; Gokhale, N. H.; Long, E. C.; Cowan, J. A. *J. Am. Chem. Soc.* **2007**, *129*, 8353.

8. Liang, Q.; Ananias, D. C.; Long, E. C. *J.Am. Chem. Soc.* **1998**, *120*, 248.

9. Lewis, M. A., Purdue University, **2007**.